

1.6 *Bistatic clutter*

1. Monostatic radar clutter
2. Clutter models
3. Bistatic clutter
4. Experimental measurements of bistatic sea clutter
5. Urban land clutter at PBR frequencies ?
6. Summary

Distributed targets

The RCS of an area-distributed target, such as the surface of the Earth is given by :

$$\sigma = \sigma^o A$$

where A is the area of the resolution cell of the radar :

$$A = \frac{c\tau}{2} \times R\theta_B$$

σ^o is dimensionless

$$\sigma^o = \frac{\sigma}{A}$$

and is usually expressed in dB (dBm²/m²)

It will depend on factors such as the angle of incidence, the dielectric properties of the surface, its roughness compared to the wavelength, and the polarisation.

Volume scattering

The reflectivity of volume clutter (such as rainfall) is characterised in terms of an RCS per unit volume η (units of $\text{m}^2/\text{m}^3 \equiv \text{m}^{-1}$).

The RCS of a single droplet is $\sigma_{drop} = C\pi^5 D^6 / \lambda^4$

where C is a dimensionless constant which is 1 for water and ~ 0.2 for ice.

To get the RCS of a rain cloud we must sum over the number of scatterers N in the volume resolution cell of the radar :

$$\sigma_{cloud} = \frac{C\pi^5}{\lambda^4} \sum_1^N D_i^6$$

We can also define :

$$Z = \sum_1^N D_i^6 / \text{unit volume} = 200r^{1.6} \quad \text{where } r \text{ is the rainfall rate (mm/hr)}$$

Radar clutter and clutter models

The value of σ^o can be used in the radar equation to calculate the mean clutter power, and hence the signal-to-clutter ratio.

But the clutter is comprised of contributions from many scatterers within the radar resolution cell, so the clutter is itself a noise process. It is therefore necessary to understand the nature of the clutter statistics in order to accurately predict the radar detection performance.

Real clutter distributions are a function of surface type (land, sea, ...), radar frequency, radar resolution, angle of incidence, polarisation, direction of radar look, etc.)

Clutter models can include the mean reflectivity (σ^o), the statistical properties, and the Doppler spectrum.

Clutter models

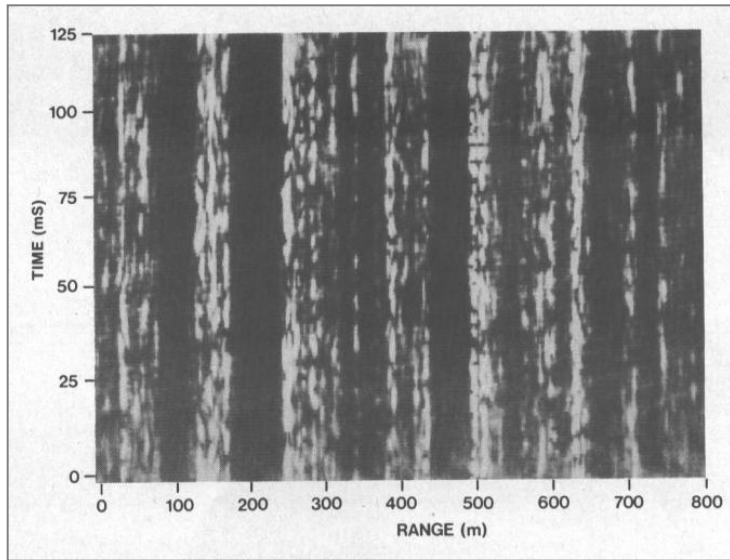
Models of clutter are required for:

- performance prediction
- comparative performance assessment
- design of detection processing
- measurement of performance for acceptance

Models may be theoretical or empirical and usually represent typical or average performance

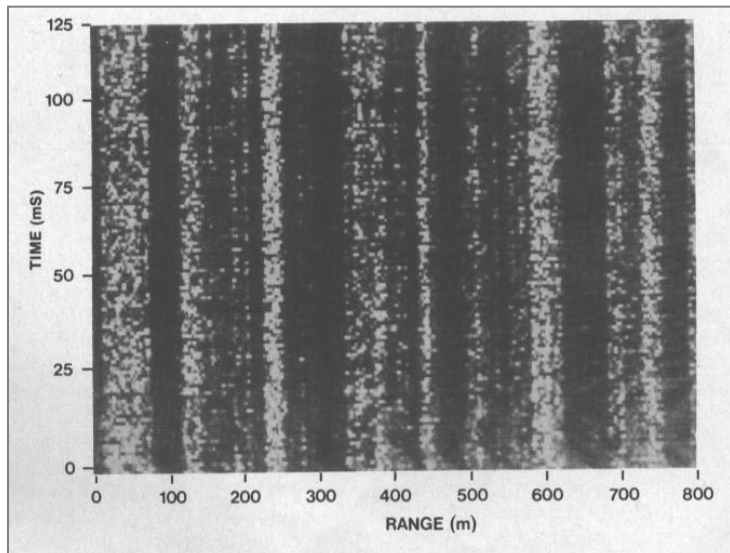
Real life on any given trial may ‘deviate’ considerably from the models

Sea clutter



Pulse by pulse clutter returns with a fixed radar frequency.

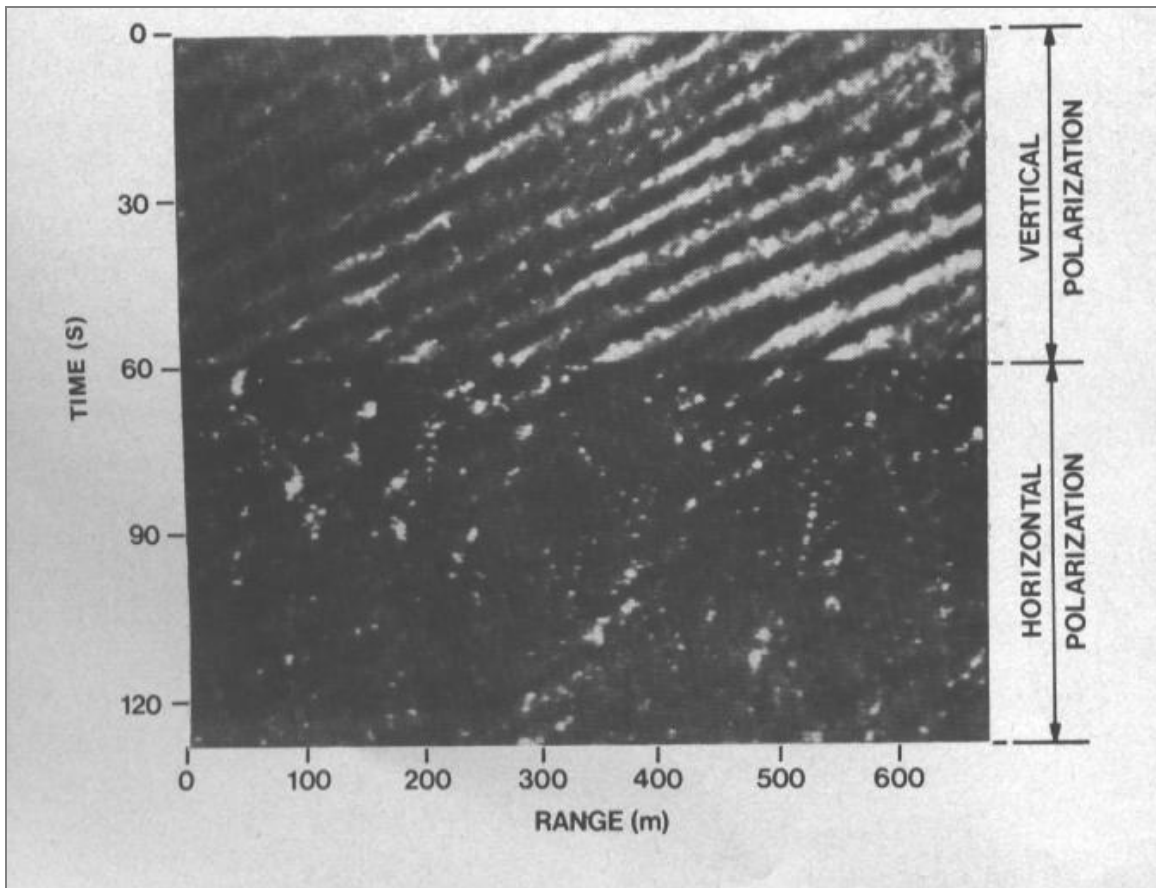
I-band clifftop radar with 1.2° beamwidth and 28 ns pulse length from a range window of 960 m at a range of 5 km, and grazing angle = 1.5°.



Pulse by pulse clutter returns with frequency agility.

From 'Radar sea clutter', K.D. Ward and S. Watts, *Microwave Journal*, June 1985, pp109-121.

Sea clutter



Range-time intensity plot of clutter, averaged to show the modulating component.

From 'Radar sea clutter', K.D. Ward and S. Watts, *Microwave Journal*, June 1985, pp109-121.

Clutter statistics

Radar clutter has been studied since the earliest days of radar. A proper knowledge of the statistics of radar clutter is essential in predicting radar detection performance, i.e. in ensuring correct setting of the detection threshold in CFAR processing, and in determining the clutter residue at the output of Doppler filter processors

For radars of low or moderate resolution, Gaussian statistics have for many years given adequate results, both for land and sea clutter. However, for high resolution radars at low grazing angles, it has been found that the clutter pdfs deviate quite markedly from Gaussian, and consequently that the detection performance predicted by Gaussian clutter models does not agree well with practical experience. This is particularly true for the ‘tails’ of the distributions, which are exactly the parts which have the greatest effect on the false alarm rate.

Furthermore, high spatial resolution radars may be able to exploit the spatial and temporal correlation properties of the clutter.

Clutter models – Rayleigh

The simplest model for radar clutter assumes that the clutter echo is the sum of a large number of contributions of similar amplitude and random phase, in which case the Central Limit Theorem indicates that the in-phase (I) and quadrature (Q) components are independent and Gaussian distributed, in which case the intensity follows a negative-exponential distribution

$$f_E(x) = \frac{1}{\beta} \exp\left(-\frac{x}{\beta}\right)$$

and the corresponding pdf of the envelope-detected voltage z is Rayleigh

$$f_R(z) = \frac{2z}{\beta} \exp\left(-\frac{z^2}{\beta}\right) \quad z \geq 0$$

Clutter models – Ricean

If there is an additional non-random component in the clutter echo, the peak of the distribution is shifted so that the most probable value of the received power is not zero. The pdf of the detected envelope can be written as:

$$f(z) = \frac{z}{\psi_0} \exp\left(-\frac{z^2 + A^2}{2\psi_0}\right) I_0\left(\frac{zA}{\psi_0}\right)$$

where $I_0(.)$ is the modified Bessel function of order zero, ψ_0 is the variance of the noise, A is the amplitude of the coherent component, and the ratio of coherent to random scattering is proportional to A^2/ψ_0 .

Clutter models – Lognormal

The lognormal distribution is obtained from the normal distribution using the transformation $x = \ln(y)$. The pdf of the detected envelope is

$$f(z) = \frac{2}{\sqrt{2\pi}\sigma z} \exp\left[-\frac{1}{2\sigma^2}\left(2\ln\frac{z}{z_m}\right)^2\right]$$

where z_m is the median value of z and σ^2 is the standard deviation of $\ln(z)$.

Clutter models – Weibull

The Weibull pdf is intermediate between the Rayleigh and lognormal distributions:

$$f_w(x) = \frac{\nu}{\beta} \left(\frac{x}{\beta} \right)^{\nu-1} \exp \left(- \left(\frac{x}{\beta} \right)^\nu \right)$$

where β is the scale parameter and ν is the shape parameter. For $\nu = 2$ the expression reduces to the Rayleigh case.

In the 1970s, much research was done on the non-Gaussian characteristics of high-resolution clutter. The lognormal distribution was found to give a better fit than the negative exponential distribution, but still fell short of describing adequately the single point statistics of coherent clutter.

Clutter models – the compound K-model

The K-distribution was originally devised in the context of optical scattering, and was subsequently applied in its compound form to radar sea clutter. It consists of the product of a modulation component associated with the large scale structure (in the case of sea clutter this represents the long-wavelength swell waves) and Rayleigh-distributed speckle resulting from the coherent addition of contributions from the individual scatterers.

More recently, the K-distribution has also been found to give a pretty accurate representation of the statistics of texture in high-resolution SAR images of rural target scenes, and even of texture in high-resolution sonar images of the seabed.

Clutter models – the compound K-model

The Rayleigh distributed speckle component is described by

$$f(x|y) = \frac{\pi x}{2y^2} \exp\left(-\frac{\pi x^2}{4y^2}\right) \quad \text{for } 0 < x < \infty$$

and the modulation component is described by the chi-distribution:

$$f(y) = \frac{2b}{\Gamma(\nu)} (b\nu)^{2\nu-1} \exp(-b^2 y^2) \quad \text{for } 0 < y < \infty$$

where b is a scale parameter and ν is a shape parameter.

Clutter models – the compound K-model

These two equations are combined to yield the usual form of the compound K-distribution:

$$f(x) = \frac{4c}{\Gamma(\nu)} (cx)^\nu K_{\nu-1}(2cx)$$

where $c = b\sqrt{\frac{\pi}{4}}$ is a scale parameter, ν is the same shape parameter as the chi-distributed modulation, and $K_\nu(\cdot)$ is the modified Bessel function of the third kind of order ν .

For $\nu = \infty$ the expression reduces to the Rayleigh distribution.

Low values of shape parameter $\nu (< 1)$ indicate spiky clutter.

Georgia Tech sea clutter model

1 – 10 GHz

Reflectivity equations:

$$\sigma_0(H) = 10 \log [3.9 \cdot 10^{-6} \lambda \psi^{0.4} G_a G_u G_w]$$

$$\sigma_0(V) = \begin{cases} \sigma_0(H) - 1.05 \ln(h_a + 0.015) + 1.09 \ln(\lambda) + 1.27 \ln(\psi + .0001) + 9.70 & \text{(3 to 10 GHz)} \\ \sigma_0(H) - 1.73 \ln(h_a + 0.015) + 3.76 \ln(\lambda) + 2.46 \ln(\psi + .0001) + 22.2 & \text{(below 3 GHz)} \end{cases}$$

where $\sigma_0(H)$ and $\sigma_0(V)$ are the reflectivities evaluated for V and H polarisations respectively.

The adjustment factors are

$$G_a = \frac{a^4}{1+a^4} \quad G_u = \exp \left[0.2 \cos \phi (1 - 2.8\psi) (\lambda + 0.015)^{-0.4} \right] \quad G_w = \left[\frac{1.94 V_w}{1+V_w/15.4} \right]^q$$

with

$$q = 1.1 / (\lambda + 0.015)^{0.4} \quad \text{and} \quad a = (14.4\lambda + 5.5)\psi h_a / \lambda$$

Georgia Tech sea clutter model

10 – 100 GHz

Reflectivity equations:

$$\sigma_0(H) = 10 \log [5.78 \cdot 10^{-6} \psi^{0.547} G_a G_u G_w]$$

$$\sigma_0(V) = \sigma_0(H) - 1.38 \ln(h_a) + 3.43 \ln(\lambda) + 1.31 \ln(\psi) + 18.55$$

where $\sigma_0(H)$ and $\sigma_0(V)$ are the reflectivities evaluated for V and H polarisations respectively.

The adjustment factors are

$$G_a = \frac{a^4}{1+a^4}$$

$$G_u = \exp [0.25 \cos \phi (1 - 2.8\psi) \lambda^{-0.33}]$$

$$G_w = \left[\frac{1.94 V_w}{1+V_w/15.4} \right]^q$$

with

$$q = 1.93 \lambda^{-0.04} \quad \text{and} \quad a = (14.4\lambda + 5.5)\psi h_a / \lambda$$

Georgia Tech sea clutter models

Units and symbols

$\sigma_0(H), \sigma_0(V)$	reflectivity for H and V polarisations, dBm ² /m ²
h_a	average wave height, m $\left(h_a \cong 4.52 \cdot 10^{-3} \cdot V_w^{2.5} \right)$
λ	radar wavelength, m
V_w	wind velocity, m/s
Ψ	grazing angle, rad
ϕ	look direction relative to wind direction, rad

Douglas Sea State

Douglas Sea State	Description	Wave height $h_{1/3}$ ft	Wind speed kts	Fetch nmi	Duration hr
1	smooth	0 – 1	0 – 6		
2	slight	1 – 3	6 – 12	50	5
3	moderate	3 – 5	12 – 15	120	20
4	rough	5 – 8	15 – 20	150	23
5	very rough	8 – 12	20 – 25	200	25
6	high	12 – 20	25 – 30	300	27
7	very high	20 – 40	30 – 50	500	30
8	precipitous	> 40	> 50	700	35

Beaufort Scale

Force	Wind (Knots)	WMO Classification	Appearance of Wind Effects	
			On the Water	On Land
0	< 1	Calm	Sea surface smooth and mirror-like	Calm, smoke rises vertically
1	1 – 3	Light Air	Scaly ripples, no foam crests	Smoke drift indicates wind direction, still wind vanes
2	4 – 6	Light Breeze	Small wavelets, crests glassy, no breaking	Wind felt on face, leaves rustle, vanes begin to move
3	7 – 10	Gentle Breeze	Large wavelets, crests begin to break, scattered whitecaps	Leaves and small twigs constantly moving, light flags extended
4	11 – 16	Moderate Breeze	Small waves 1 – 4 ft. becoming longer, numerous whitecaps	Dust, leaves, and loose paper lifted, small tree branches move
5	17 – 21	Fresh Breeze	Moderate waves 4 – 8 ft taking longer form, many whitecaps, some spray	Small trees in leaf begin to sway
6	22 – 27	Strong Breeze	Larger waves 8 – 13 ft, whitecaps common, more spray	Larger tree branches moving, whistling in wires
7	28 – 33	Near Gale	Sea heaps up, waves 13 – 20 ft, white foam streaks off breakers	Whole trees moving, resistance felt walking against wind
8	34 – 40	Gale	Moderately high (13 – 20 ft) waves of greater length, edges of crests begin to break into spindrift, foam blown in streaks	Whole trees in motion, resistance felt walking against wind
9	41 – 47	Severe Gale	High waves (20 ft), sea begins to roll, dense streaks of foam, spray may reduce visibility	Slight structural damage occurs, slate blows off roofs
10	48 – 55	Storm	Very high waves (20 – 30 ft) with overhanging crests, sea white with densely blown foam, heavy rolling, lowered visibility	Seldom experienced on land, trees broken or uprooted, "considerable structural damage"
11	56 – 63	Violent Storm	Exceptionally high (30 – 45 ft) waves, foam patches cover sea, visibility more reduced	
12	> 64	Hurricane	Air filled with foam, waves over 45 ft, sea completely white with driving spray, visibility greatly reduced	

Beaufort Scale Force 2



BEAUFORT FORCE 2
WIND SPEED: 4-6 KNOTS

SEA: WAVE HEIGHT .2-.3M (.5-1FT), SMALL WAVELETS,
CRESTS HAVE A GLASSY APPEARANCE AND DO NOT BREAK

Beaufort Scale Force 6



BEAUFORT FORCE 6
WIND SPEED: 22-27 KNOTS

*SEA: WAVE HEIGHT 3-4M (9.5-13 FT),
LARGER WAVES BEGIN TO FORM, SPRAY IS PRESENT,
WHITE FOAM CRESTS ARE EVERYWHERE*

Beaufort Scale Gale Force 8



BEAUFORT FORCE 8
WIND SPEED: 34-40 KNOTS

SEA: WAVE HEIGHT 5.5-7.5M (18-25FT), MODERATELY HIGH WAVES OF GREATER LENGTH, EDGES OF CREST BEGIN TO BREAK INTO THE SPINDRIFT, FOAM BLOWN IN WELL MARKED STREAKS ALONG WIND DIRECTION.

Beaufort Scale Hurricane Force 12



BEAUFORT FORCE 12
WIND SPEED: 64 KNOTS

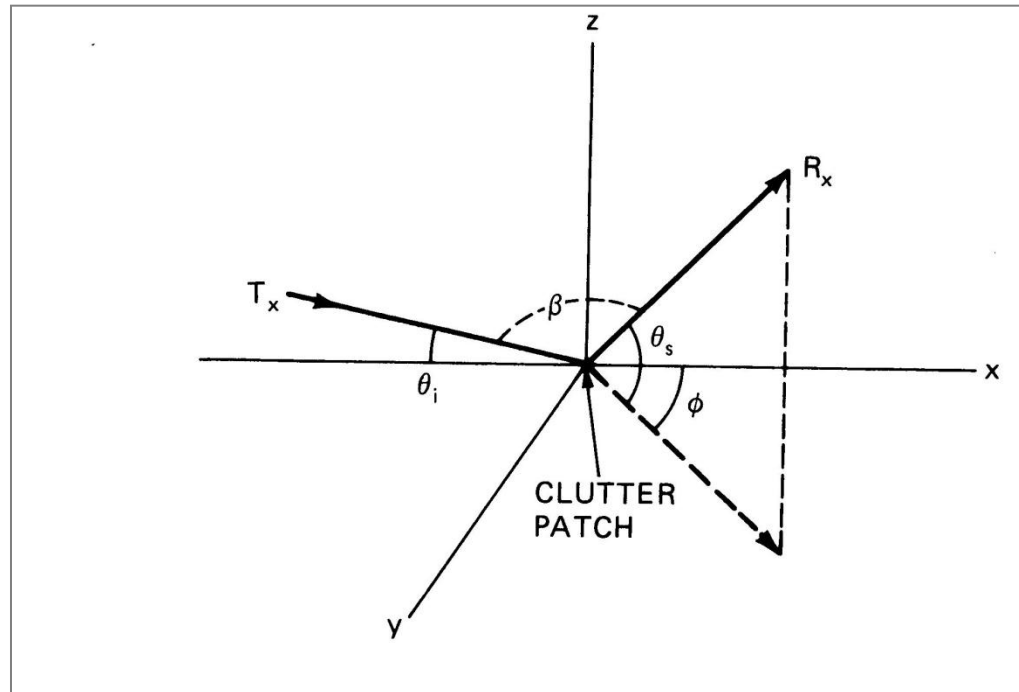
SEA: SEA COMPLETELY WHITE WITH DRIVING SPRAY,
VISIBILITY VERY SERIOUSLY AFFECTED. THE
AIR IS FILLED WITH FOAM AND SPRAY

On bridge wing - HMS Beaver, GRIUK Gap

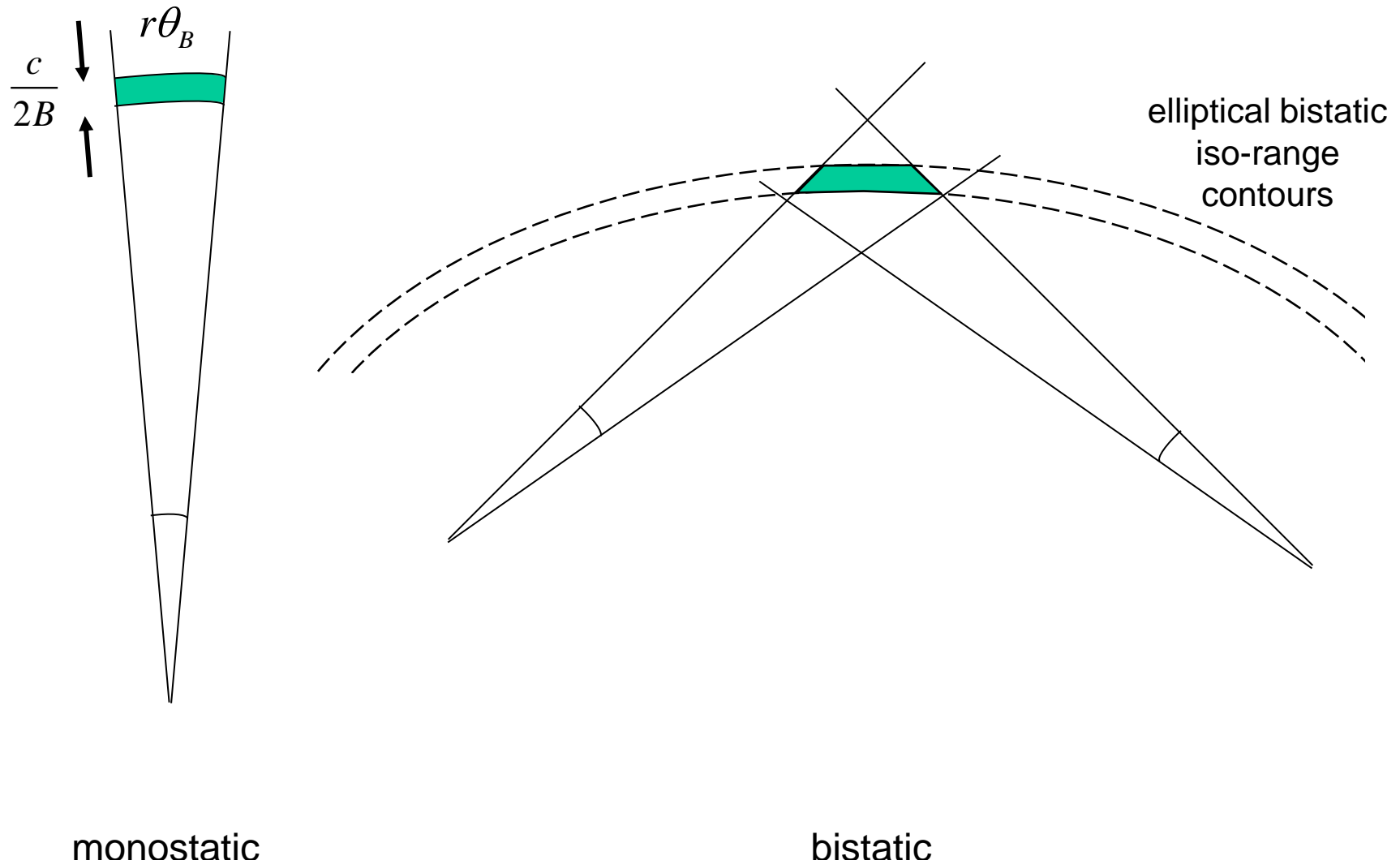


Bistatic clutter

- All of the parameters associated with monostatic clutter – plus geometry
- Little data exists
- Maximum at specular reflection ('specular ridge') and at forward scatter



Clutter cell area



monostatic

bistatic

Clutter cell area

M = Main lobe clutter

S = Sidelobe clutter

xxxxxx M_A, M_B

||||||| S_B, M_A, OR S_A, M_B

— S_A, S_B

••••• Beyond receiver line of sight

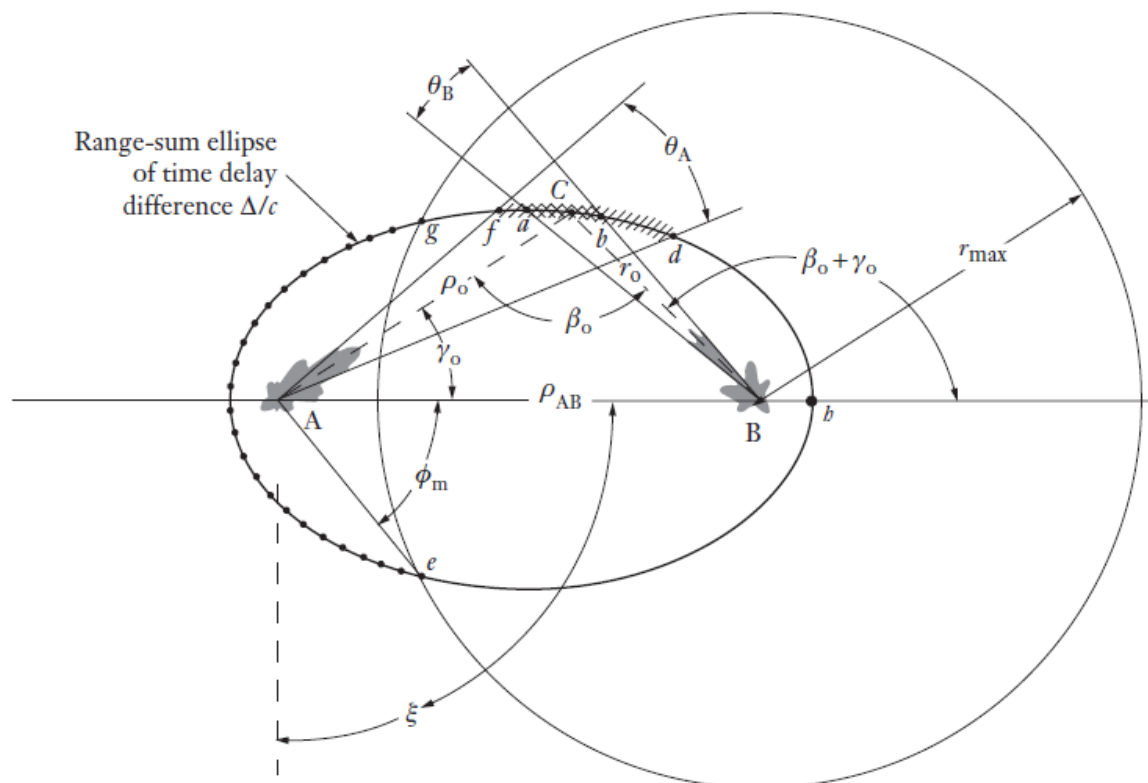
A = Transmitter

B = Receiver

C = Clutter cell

$$(M_A, M_B)$$

$$\Delta = \rho_0 + r_0 - \rho_{AB}$$



Bistatic clutter

organization	authors	surface	frequency	polarization	θ_i	θ_s	ϕ
Ohio State University (1965)	Cost, Peakes	smooth sand, loam, soybeans; rough sand, loam with stubble, grass	10 GHz	VV, HH	5 – 30°	5 – 30°	0 – 145°
				HV	10 – 70°	5 – 90°	0, 180°
					5 – 70°	5 – 90°	0, 180°
Johns Hopkins University (1966-67)	Pidgeon	sea (sea states 1, 2, 3)	C-band,	VV, VH	0.2 – 3°	10 – 90°	180°
		sea (Beaufort wind 5)	X-band	HH	1 – 8°	12 – 45°	180°
GEC Stanmore (1967)	Domville	rural land, urban land, sea (20 kt wind)	X-band	VV, HH	6 – 90° ≈ 0 – 90°	6 – 180° ≈ 0 – 180°	180, 165° 180, 165°
University of Michigan (ERIM) (1978)	Larson, Heimiller	Semidesert, grass with cement taxiway, weeds and scrub trees	1.3 and 9.4 GHz	HH, HV	≈ 0	?	180, 165°
					10, 40°	5, 10, 20°	0 – 180°
					10, 15, 20°		0 – 105°
Georgia Institute of Technology (1982-84)	Ewell, Zehner	Sea (0.9, 1.2 – 1.8 m wave heights)	9.38 GHz	VV, HH	≈ 0	≈ 0	90 – 160°
University of Michigan (EECS) (1988)	Ulaby et al.	smooth sand rough sand gravel	35 GHz	VV, HH VH, HV	24°	24°	0 – 170°
					30°	30°	0 – 170°
					30°	10 – 90°	0 – 90°

Bistatic clutter

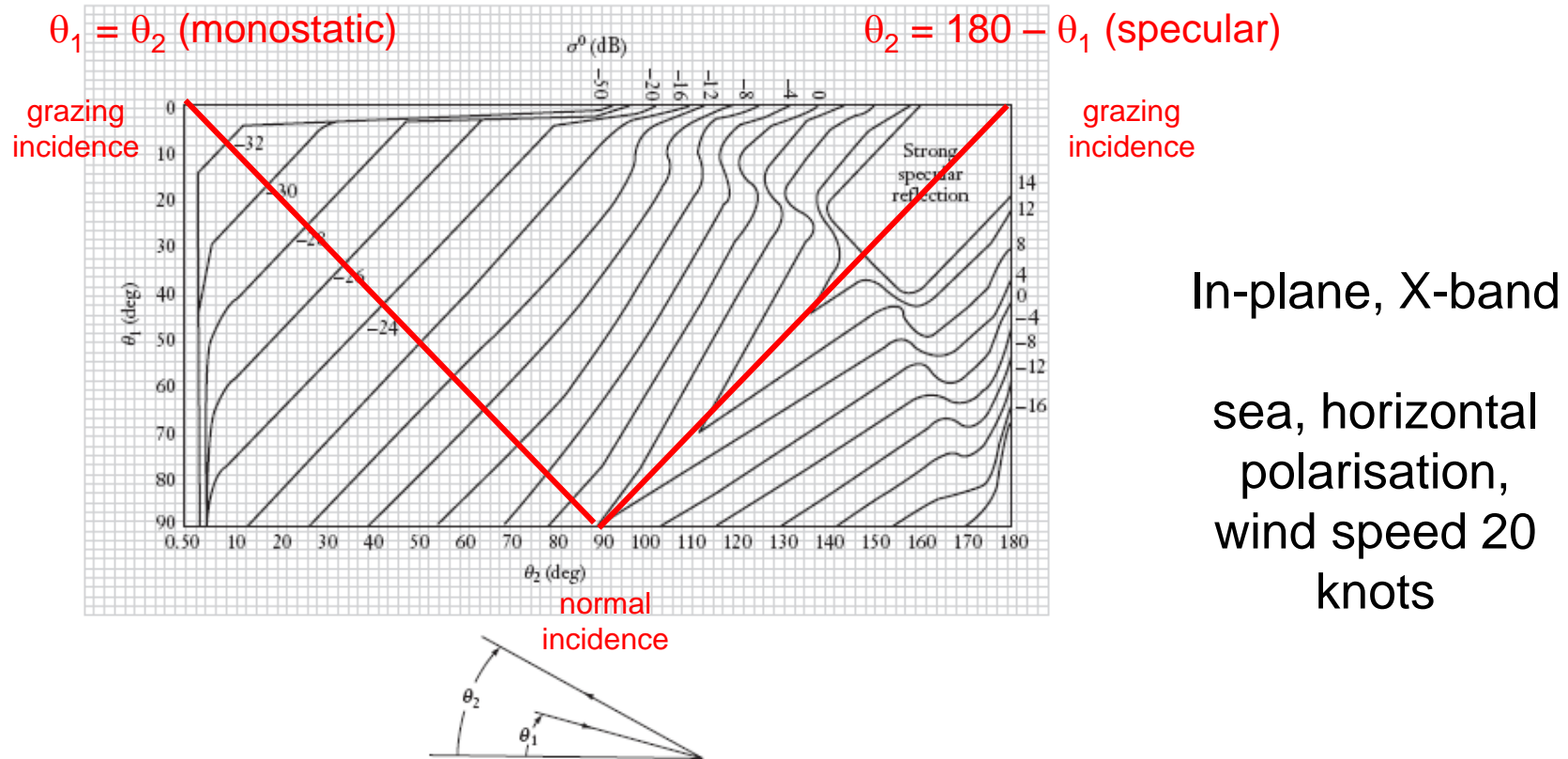
organization	authors	surface	frequency	polarization	θ_i	θ_s	ϕ
Ohio State University (1965)	Cost, Peakes	smooth sand, loam, soybeans; rough sand, loam with stubble, grass (dry/damp/snow cover)	10 GHz	VV, HH HV	5 – 30° 10 – 70° 5 – 70°	5 – 30° 5 – 90° 5 – 90°	0 – 145° 0, 180° 0, 180°
Johns Hopkins University (1966-67)	Pidgeon	sea (sea states 1, 2, 3) sea (Beaufort wind 5)	C-band, X-band	VV, VH HH	0.2 – 3° 1 – 8°	10 – 90° 12 – 45°	180° 180°
GEC Stanmore (1967-69)	Domville	rural land, urban land, forest, sea (20 kt wind), semidesert, wet	X-band	VV, HH	6 – 90° \approx 0 – 90°	6 – 180° \approx 0 – 180°	180, 165° 180, 165°
University of Michigan (ERIM) (1978-79)	Larson, Heimiller	Flat grass with cement axiway, weeds and scrub trees Snow covered orchard, snow –covered weed and scrub trees	1.3 and 9.4 GHz	HH, HV	\approx 0 10, 40° 10, 15, 20°	?	180, 165° 0 – 180° 0 – 105°
Raytheon Co., Wayland, MA	Cornwell, Lancaster	beach with sand dunes. ocean, sea state 2	9.1 GHz	VV	0	unspec'd low grazing angles	

Bistatic clutter (ii)

organization	authors	surface	frequency	polarization	θ_i	θ_s	ϕ
Georgia Inst of Technology (1982-84)	Ewell, Zehner	Sea (0.9, 1.2 – 1.8 m wave heights)	9.38 GHz	VV, HH	5 – 30°	5 – 30°	0 – 145°
				HV	10 – 70°	5 – 90°	0, 180°
					5 – 70°	5 – 90°	0, 180°
University of Michigan (EECS) (1988)	Ulaby et al	smooth sand rough sand, gravel	35 GHz	VV, HH	0 - 170°	66°	9 - 132°
				VH, HV	0 - 170°	66°	9 - 120°
					0 - 90°	60°	48 - 140°
MIT Lincoln Labs (1992)	Kochanski et al.	sea (sea state 1)	10 GHz	HH, VV	0.2 – 3°	10 – 90°	180°
					1 – 8°	12 – 45°	180°
Northeastern University, U. Mass (1994 -2002)	McLaughlin et al.	forested hills	S-band	VV, HH VH, NV	20 - 70°	low grazing angles	110 – 160°
				2.71 GHz	Fully polarimetric	28 - 66°	low grazing angles
							114 – 152°

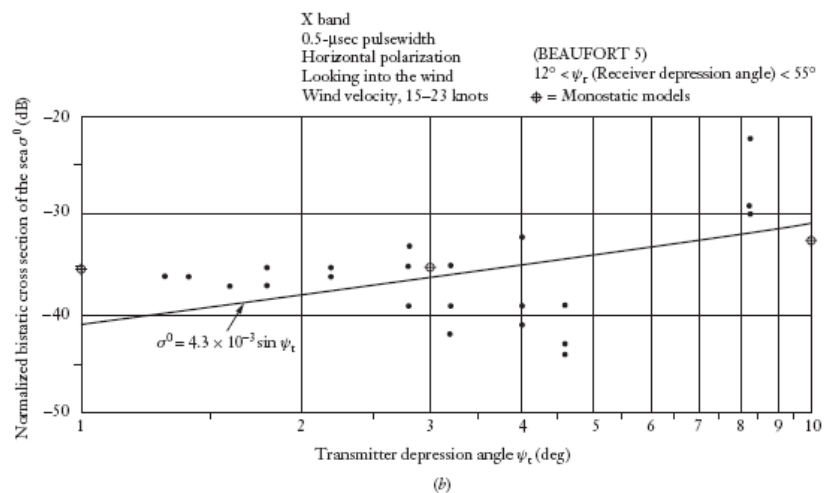
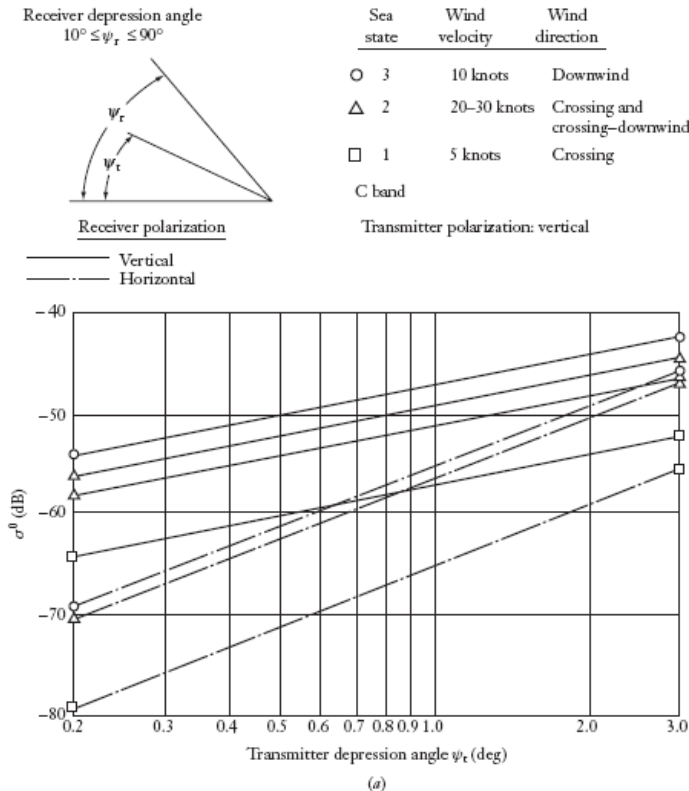
Adapted from Weiner, M, 'Clutter', chapter 9 in *Advances in Bistatic Radar*, Scitech, 2007.

Bistatic clutter



Domville, A.R., 'The bistatic reflection from land and sea of X-band radio waves', GEC (Electronics) Ltd., Memo SLM 1802, Stanmore, England, July 1967.

Bistatic clutter



Bistatic scattering coefficient of the sea in the plane of incidence at C- and X-bands (after F.E. Nathanson, Johns Hopkins University data, *Radar Design Principles*, McGraw-Hill, New York, pp88-89, 1969).

Bistatic clutter

	<u>Forward Scattering</u>	<u>Back Scattering</u>
Absolute error ± 3 dB	F.m.s. detector, sea Median level detector, land Vertical Polarization	Absolute error ± 4 dB. Median Level Detector Vertical Polarization only
Horizontal Polarisation		
$\rho_h = -0.46\theta_t - 0.39\phi$ $\pm 0.15\theta_t \pm 0.13\phi$	If $\theta_t = 0$ to 12 $\rho_v = -1.13\theta_t - 0.33\phi$ $\pm 0.17\theta_t \pm 0.14\phi$	$\sigma_0 = -47 + 1.5W + (6 - a) + \beta \pm 5$ $\beta = +4$ for down wind, 0 for into wind, -4 for cross wind
$\theta_t = 0 \rightarrow 30$ Sea $\phi = 0 \rightarrow 30$	If $\theta_t = 12$ to 30 $\rho_v = -14.1 - 0.33\phi$ $\pm 2 \pm 0.14\phi$ $\phi = 0 \rightarrow 40$	$\theta_t = 9 \rightarrow 23$ $\theta_v = 10 \rightarrow 30$ $a = 0 \rightarrow 11$ $W = 3 \rightarrow 20$
Land	$\rho = B_0 + B_2(\Delta\theta)^2 - 0.45a \pm 0.1a$ For Forest see Section 6.2.1.	Forest $\sigma_0 = -21.5 + 0.23(\theta_m - 17.5) + 0.23(\theta_b - 4)$ Rural $\sigma_0 = -20 + 0.23(\theta_m - 15.5) + 0.2(\theta_b - 5) \pm 1.8$ Urban $\sigma_0 = -19 + 0.16(\theta_m - 13) + 0.27(\theta_b - 4) \pm 3.2$ $\theta_m = 4 \rightarrow 30$ $\theta_b = 0 \rightarrow 9$ No azimuth measurements
No measurements	Rural If $\theta_t = 0$ to 22 $B_0 = -1.25\theta_t \pm 2.7$ Urban If $\theta_t = 22$ to 40 $B_0 = -27.5 \pm 2.7$ $B_2 = -0.058 + 0.001\theta_t \pm 0.01$ $\theta_t = 6 \rightarrow 40$	

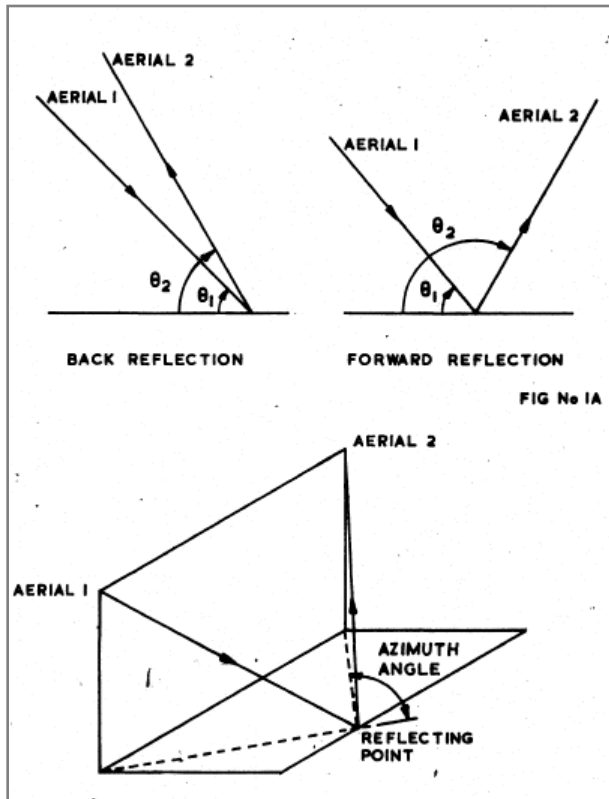
Bistatic clutter

Terrain and Polarisation	Mono or Bistatic	Range of angles see Figure 3	Source see Ref.No.	Spread of raw data dB	Deviation of smoothed data from algorithm dB	Notes
Sea Horizontal	Monostatic	H	6	2.4	0	2
	Bistatic	G	5	3.7	1.9	1
	Bistatic	D	4	1.6	1.4	3
Sea Vertical	Bistatic	G	5	2.4	3.0	1
	Monostatic	H	6	1.4	1.4	4
	Bistatic	D	4	1.1	2.4	3
Rural Vertical	Bistatic	A	1	2.5	1.5	
	Bistatic	E	5	2.9	1.6	1
	Monostatic	F	-	-		
	Bistatic	D	4	2.1	0.8	3
Forest Vertical	Bistatic	A	1	2.6	0.6	
	Bistatic	E	5	2.2	0.9	1
	Monostatic	A	1	-		
	Bistatic	C	3	2.1	2.6	5
Urban Vertical	Bistatic	A	1	4.5	1.9	
	Monostatic	A	1	-	3.3	
	Bistatic	D	4	1.5	2.4	3

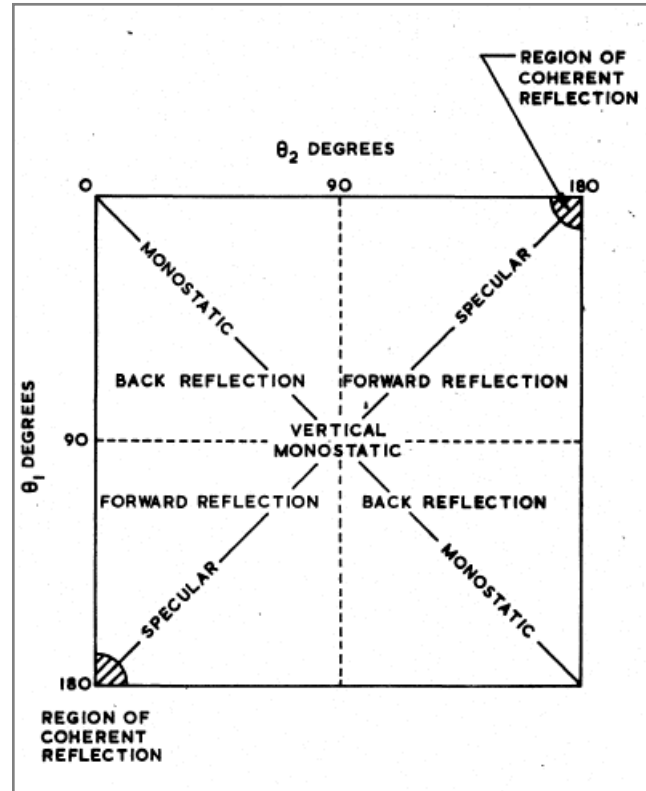
NOTES

1. Measurements with vertical illumination. In the case of Rural terrain, three suspect points from the raw data were not included, and for Forest two were not included.
2. Regression line of raw data used for this algorithm.
3. Figure for the spread obtained only from data close to the specular angle.
4. The bistatic A5 measurements are not included in the spread of the raw data.
5. The A5 measurements at an angle of 140° (depression angle 40°) were excluded as being suspect (see Reference 3). The figures given in column 6 were obtained from smoothed data taken at 10° intervals in the area 150° to 168° and 150° to 174° .

Bistatic clutter



geometry

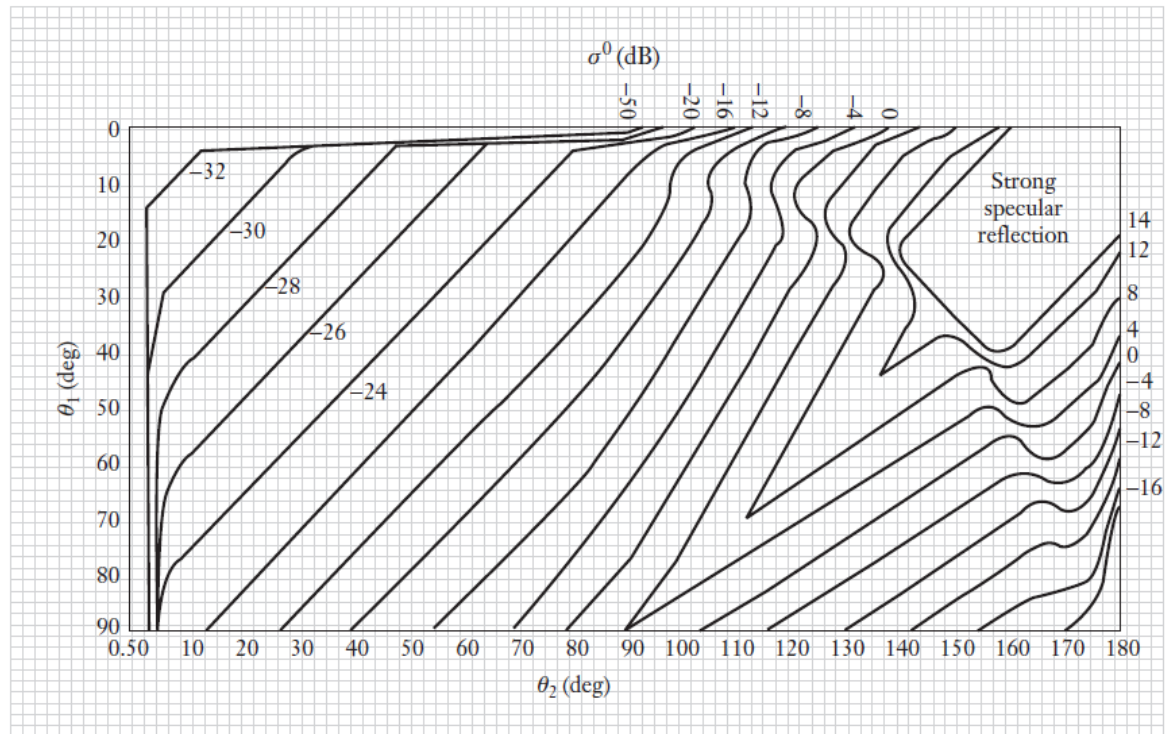


ground plane for maps of
the scattering coefficient

Domville, A.R., 'The bistatic reflection from land and sea of X-band radio waves', GEC (Electronics) Ltd., Memo SLM 1802, Stanmore, England, July 1967.

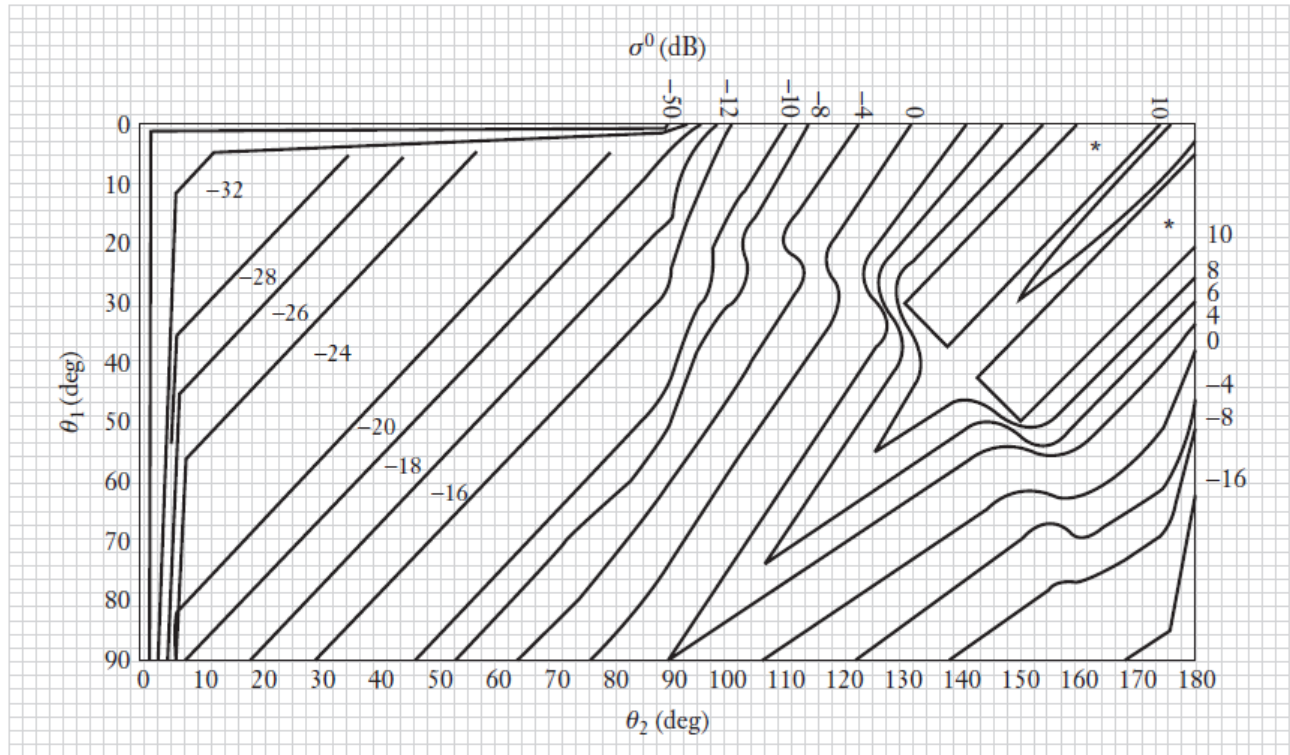
Bistatic clutter

sea, HH polarisation,
wind speed 20 knots



Bistatic clutter

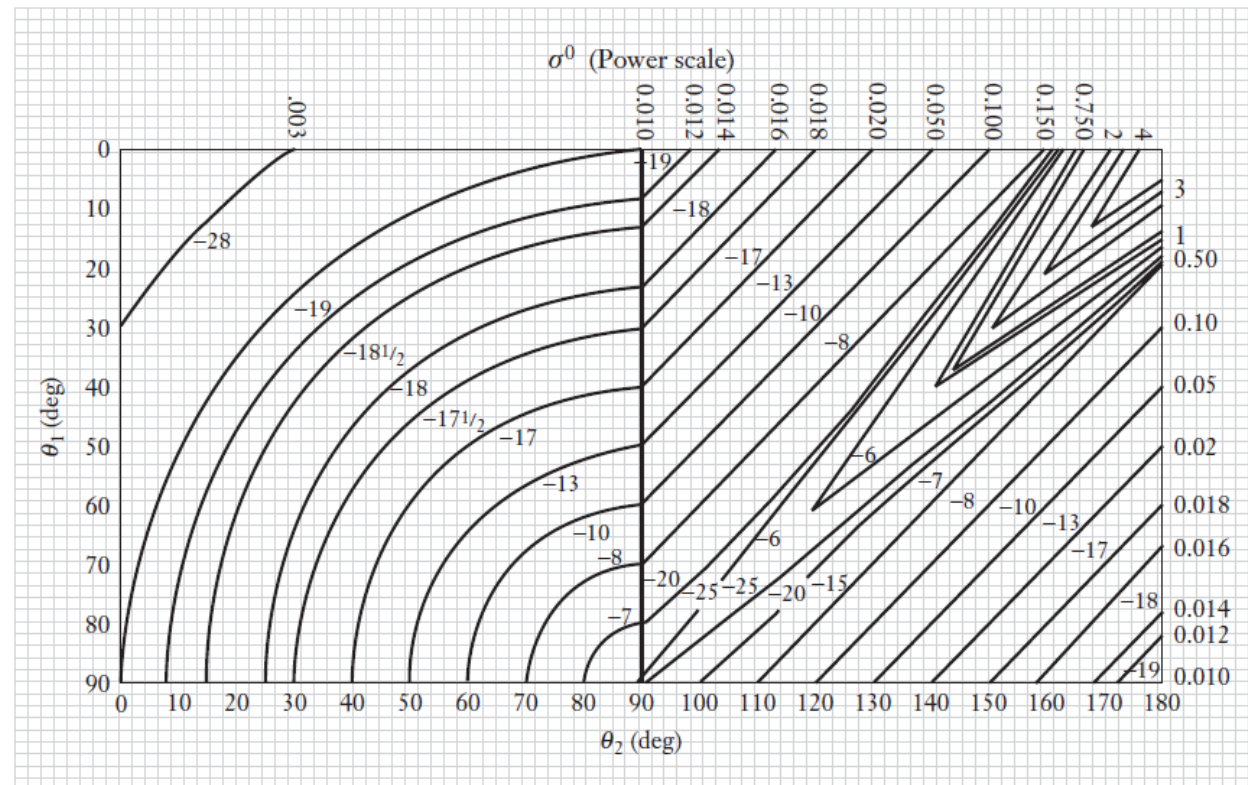
sea, VV polarisation,
wind speed 20 knots



Domville, A.R., 'The bistatic reflection from land and sea of X-band radio waves', GEC (Electronics) Ltd.,
Memo SLM 1802, Stanmore, England, July 1967.

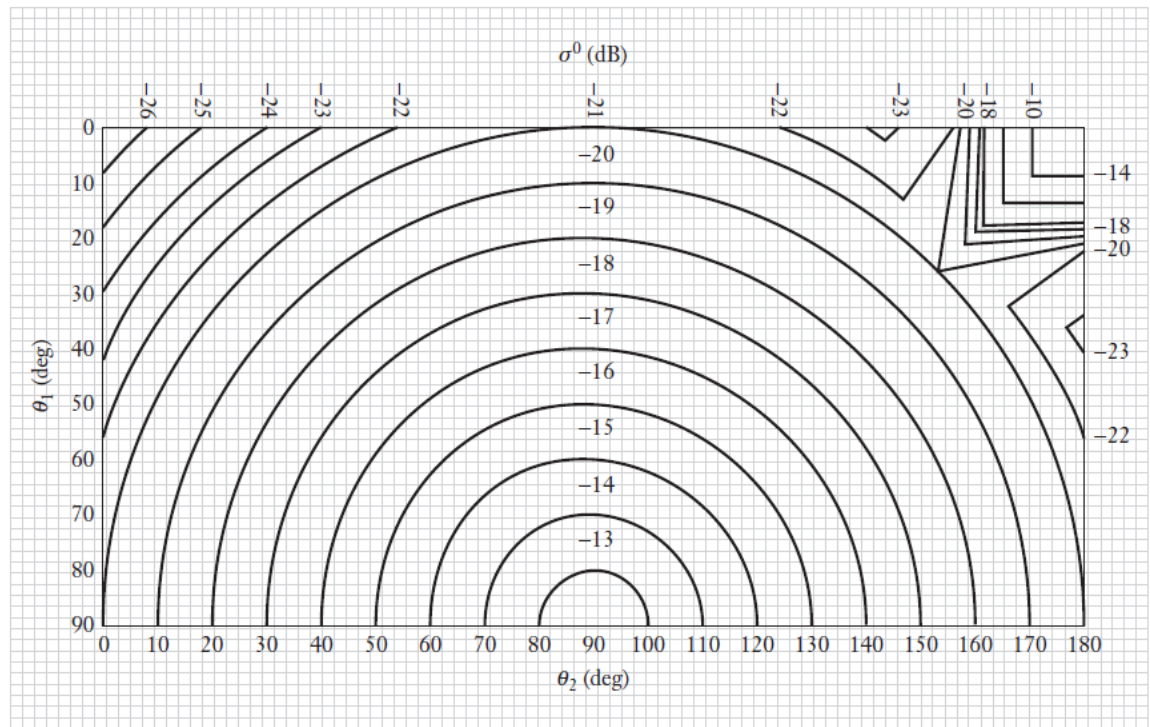
Bistatic clutter

rural land,
VV polarisation



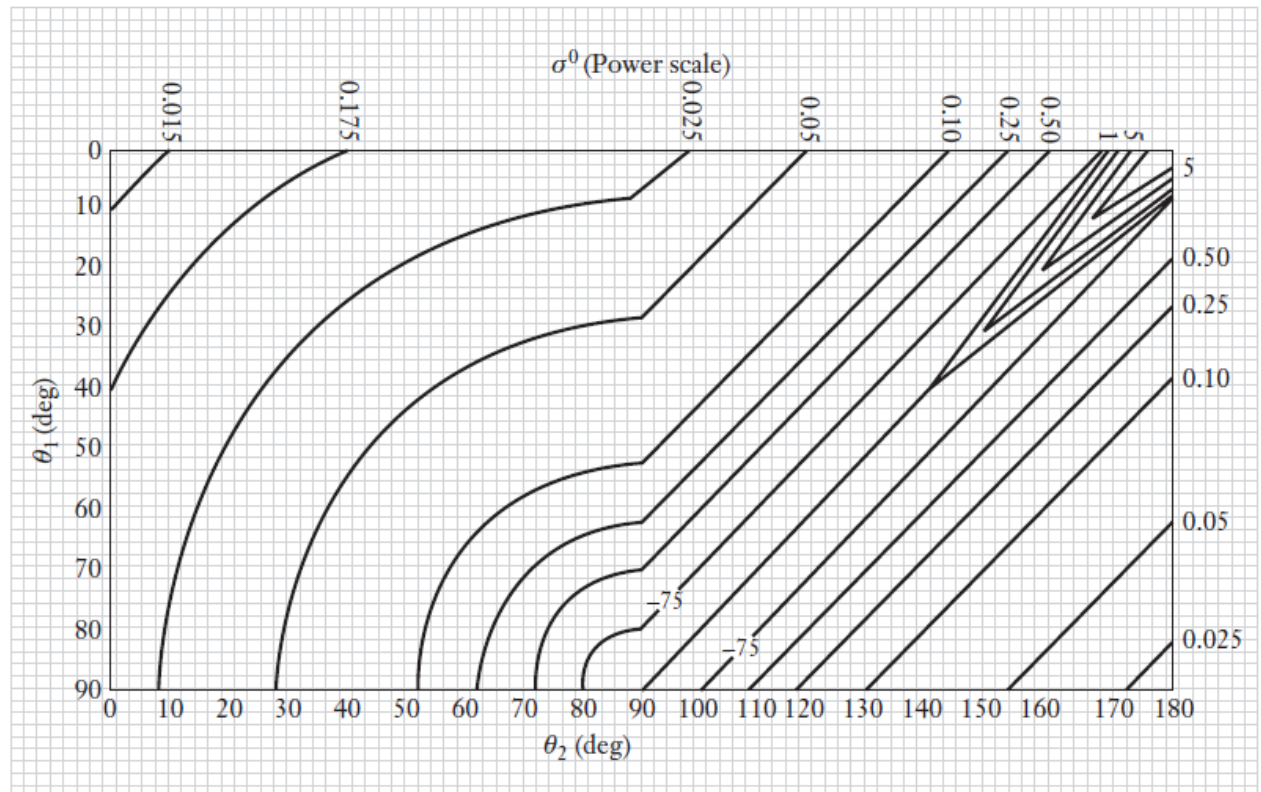
Bistatic clutter

forest,
VV polarization



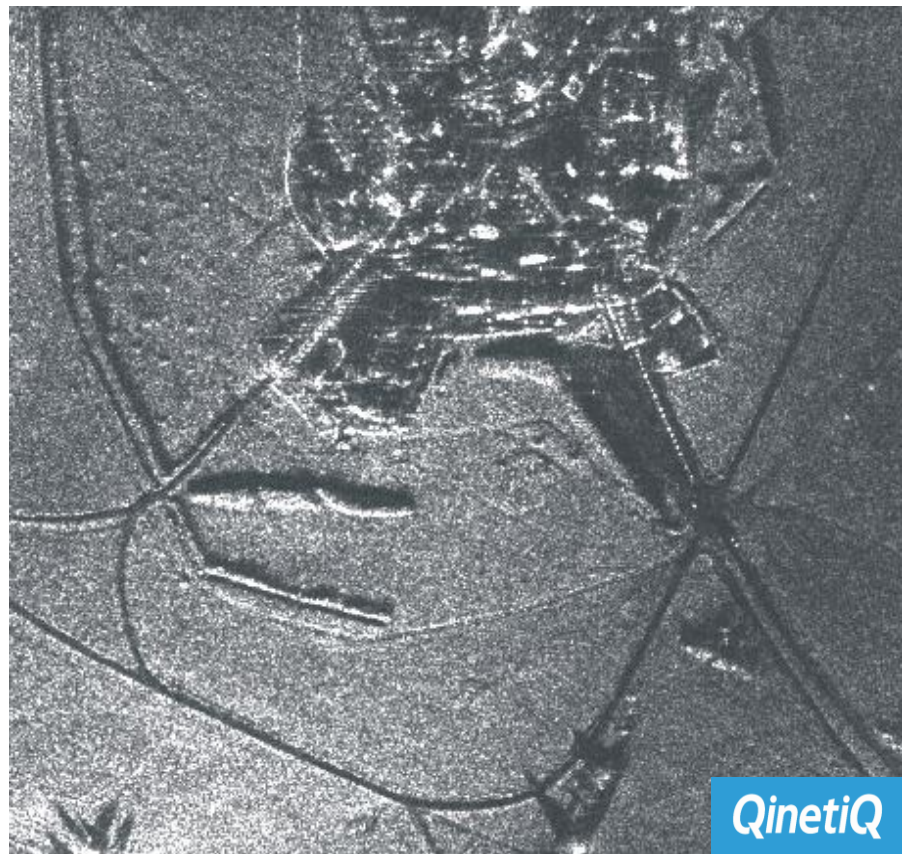
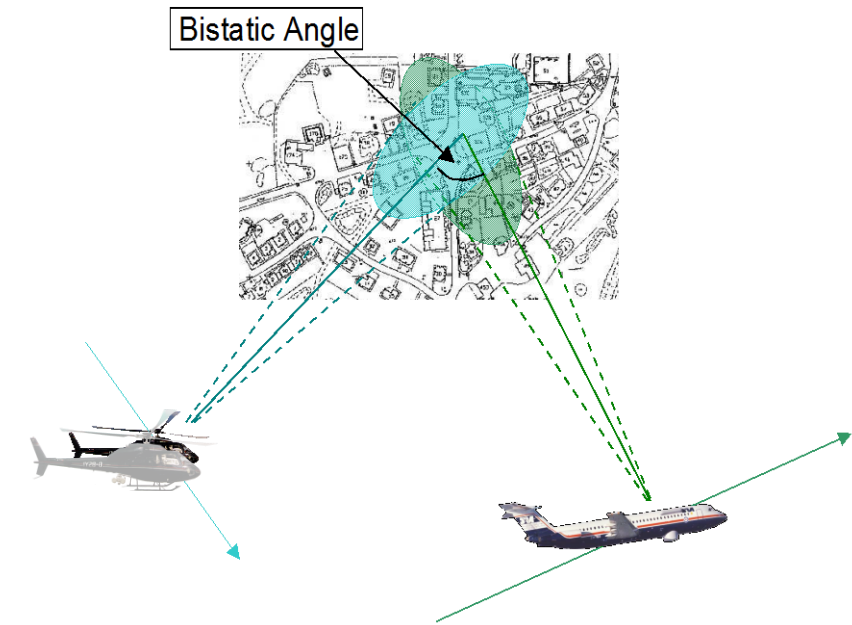
Bistatic clutter

urban land,
VV polarisation



Domville, A.R., 'The bistatic reflection from land and sea of X-band radio waves', GEC (Electronics) Ltd.,
Memo SLM 1802, Stanmore, England, July 1967.

Bistatic SAR image

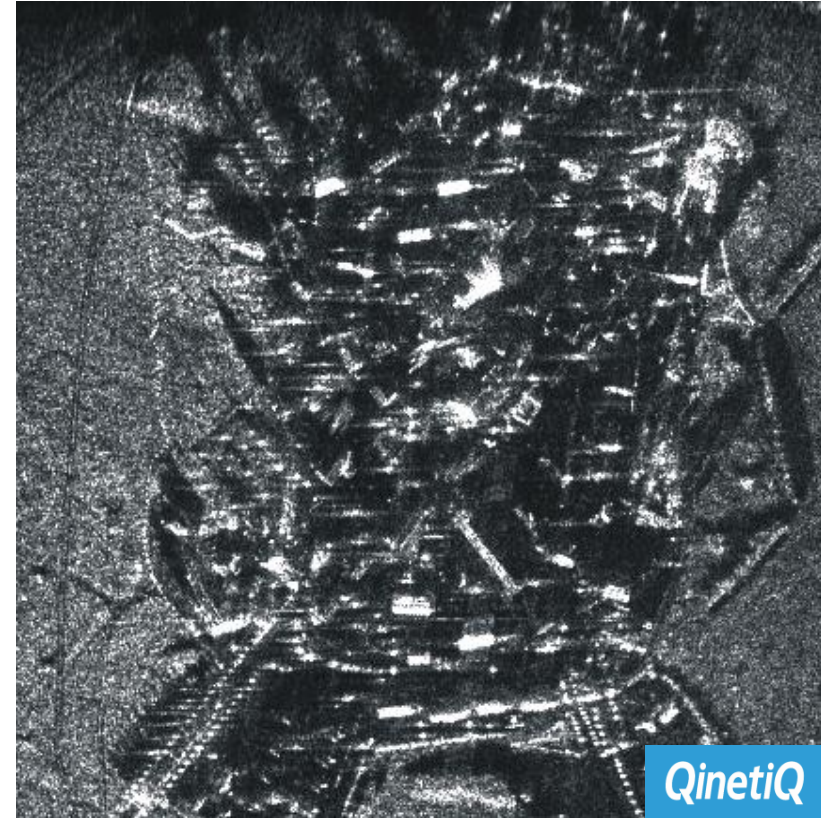


Bistatic angle $\sim 50^\circ$

Comparison of monostatic and bistatic SAR



Monostatic



Bistatic
(~70°)

QinetiQ

QinetiQ

Bistatic clutter

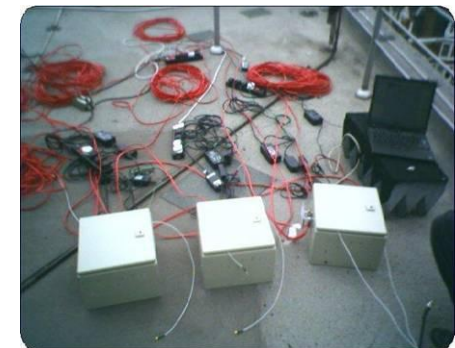
It might be expected that bistatic clutter should be less ‘spiky’ since dihedral and trihedral reflectors will not give strong reflections in bistatic geometries.

Very little experimental data exists – but results from bistatic imagery of urban target scene show higher values of K-distribution shape parameter ν for bistatic geometry.

	monostatic		bistatic	
	fit	ν	fit	ν
field 1	16%	4.27	80%	10.01
field 2	72%	6.02	58%	6.25
field 3	46%	4.10	44%	5.64

NetRAD: a multistatic radar system

Carrier frequency	2.4 GHz
Peak transmitted power	23 dBm
Maximum range over which data is recorded	3000 m
Antenna beamwidth	$8^\circ \times 8^\circ$
Maximum bandwidth	50 MHz
Nominal range resolution	3 m
Pulse lengths	0.1 – 10 μ s
Available transmissions	Chirp, Barker code, Pulse, Polyphase / Deng codes, Passive, Continuous
PRF	50 Hz – 3 kHz
Maximum number of pulses	1500

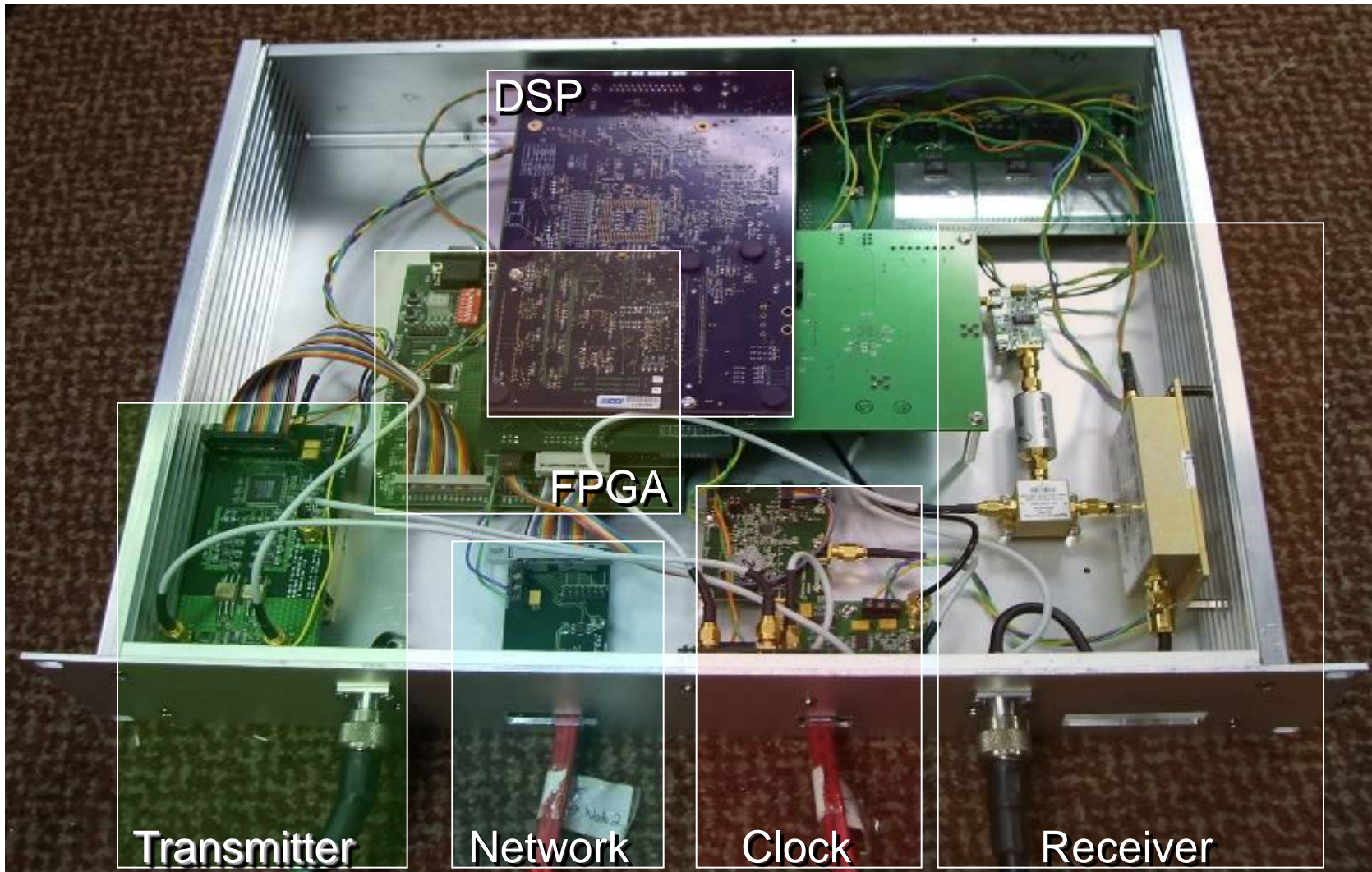


The current radar network consists of three nodes where two nodes are connected to a central node with 50 m network cables.

A 100 MHz reference oscillator is also distributed to all three nodes via three 50 m cables.

The user interface to the system is by a PC connected via parallel port to the DSP card. When outdoors, the system is powered by 65 Ah lead-acid battery.

Multistatic radar system node

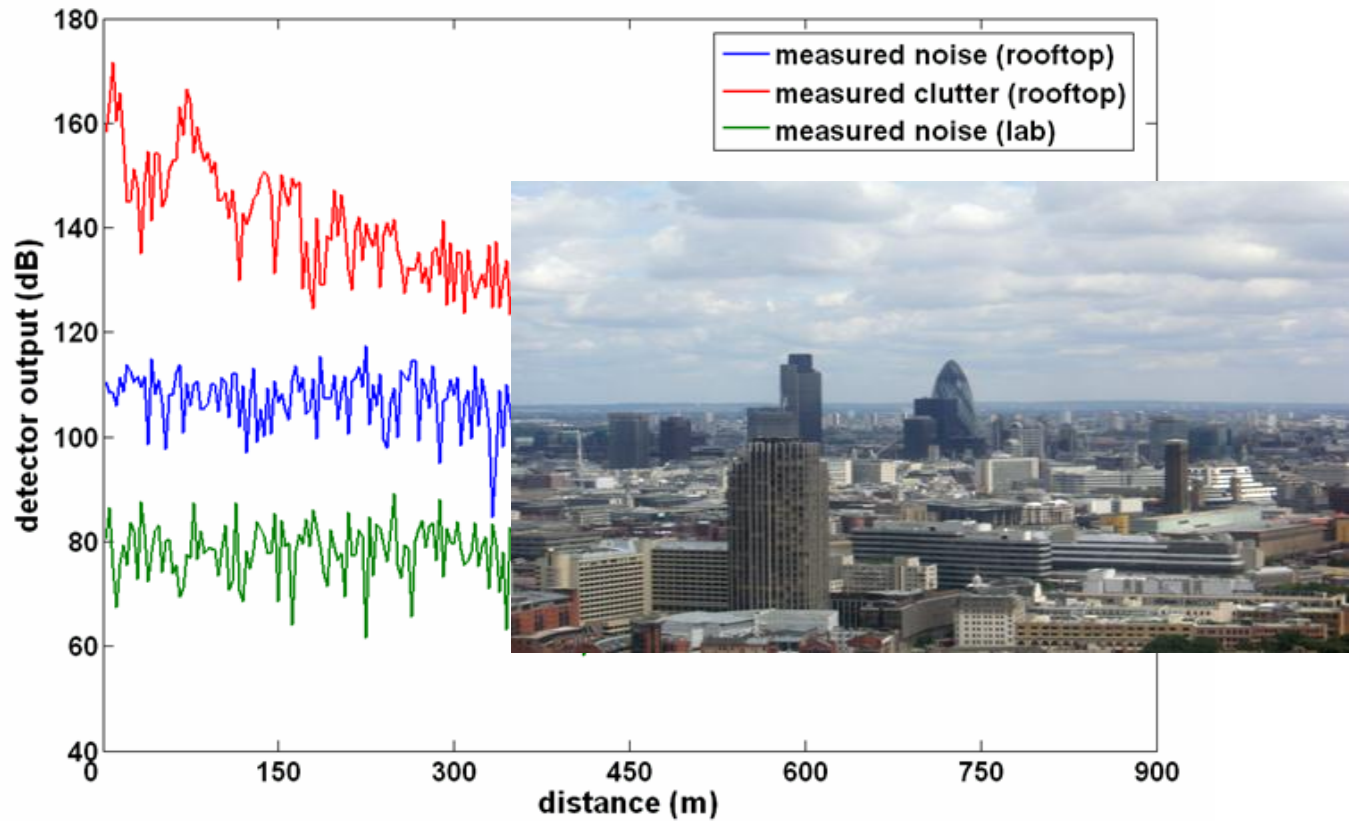


Initial monostatic testing

Initial tests were taken in an urban clutter environment, in the area surrounding UCL

Both noise and clutter measurements were taken

Typical range profile



Initial monostatic testing

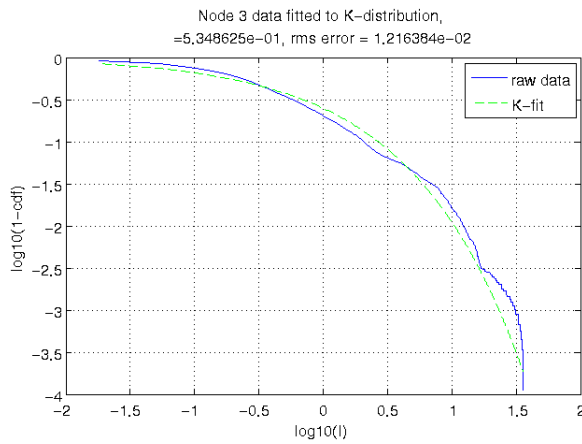


Kings Cross development

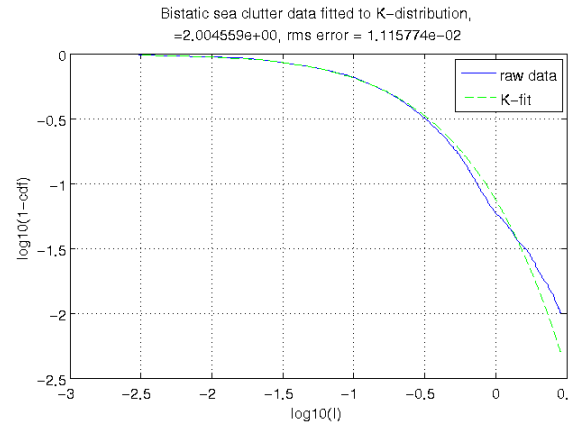
Barbican complex

Proving trials, Peacehaven, July/August 2010

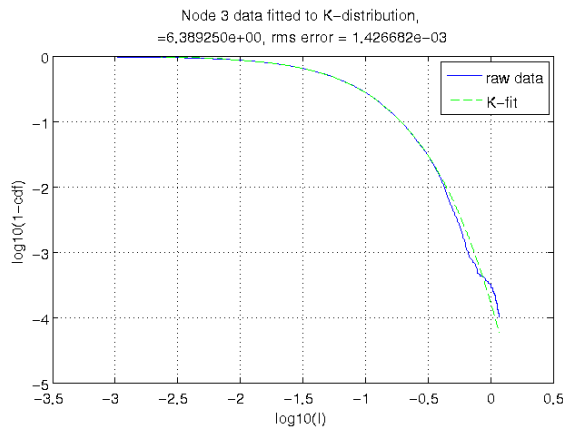




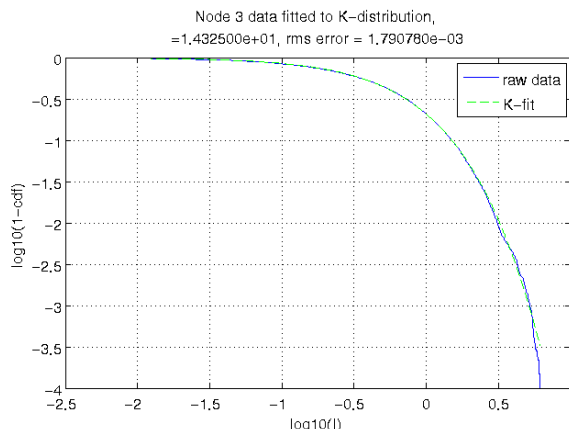
HH - monostatic, $v = 0.5$



HH - bistatic, $v = 2.0$



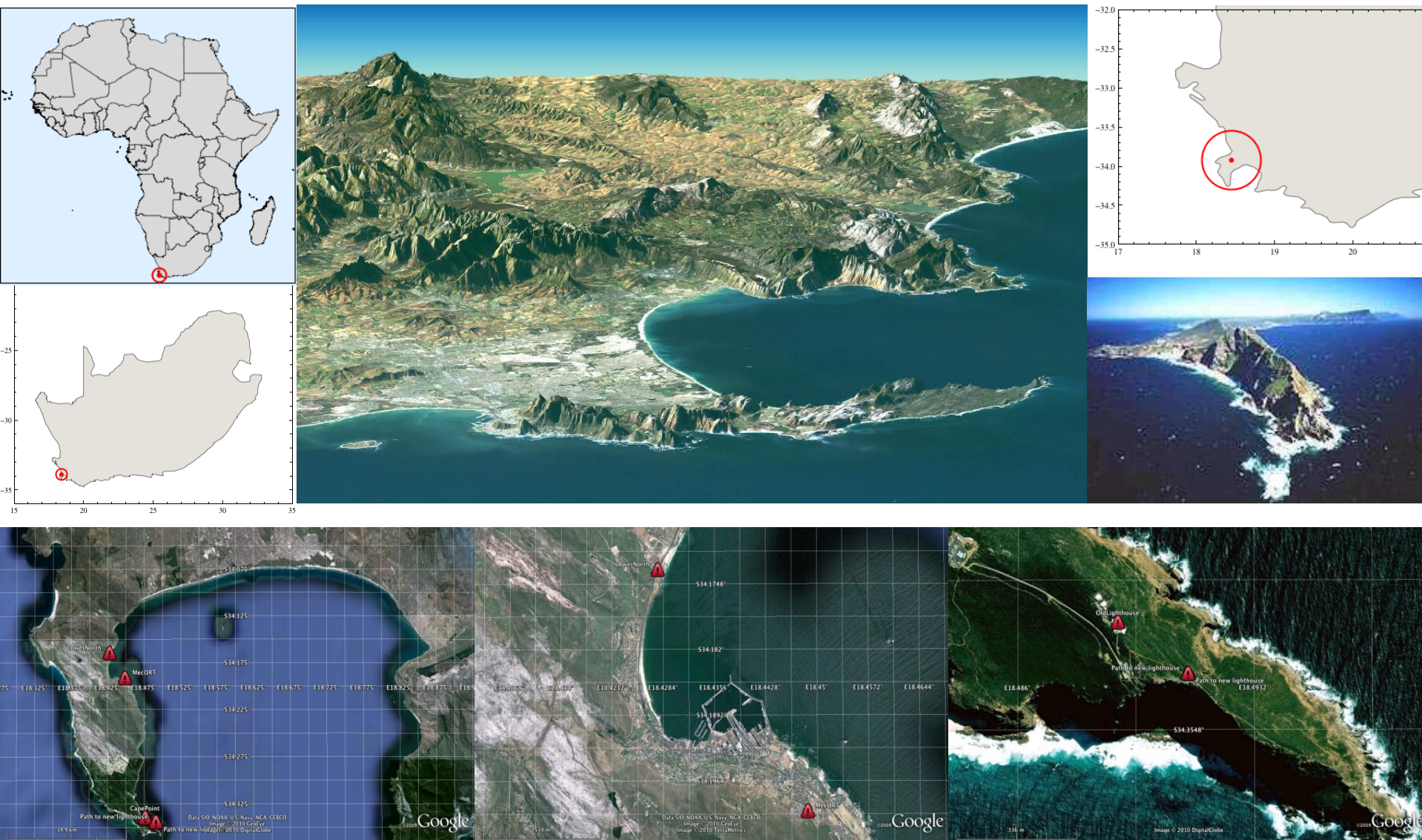
VV - monostatic, $v = 6.39$



VV - bistatic, $v = 14.35$

wind speed 13 kts (westerly), $H_{1/3} = 0.4$ m, bistatic angle = 17°

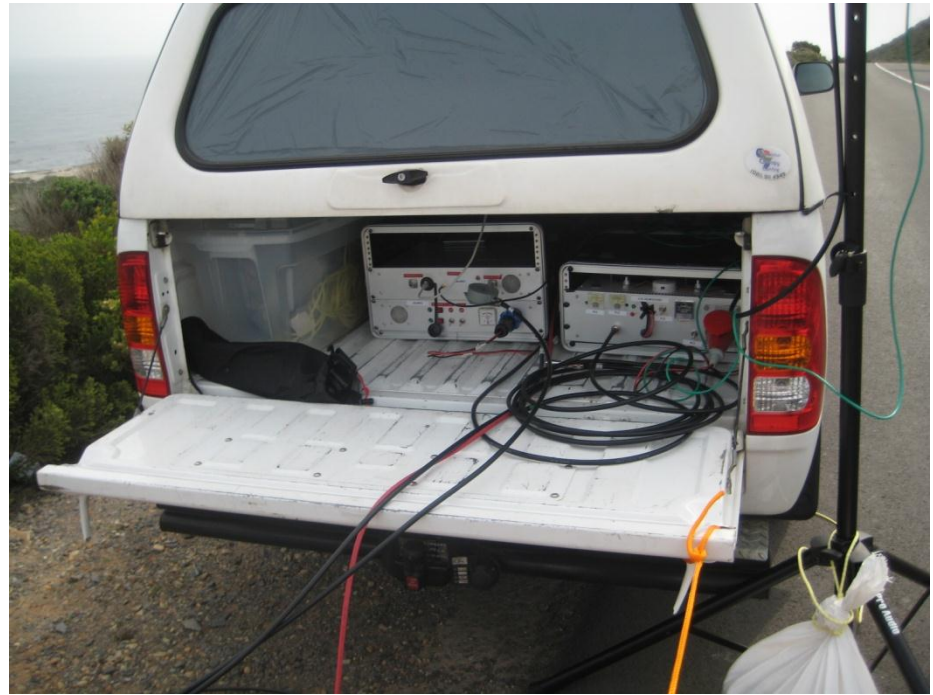
Why South Africa ?



Bistatic clutter trials: Cape Point



Bistatic clutter trials: Cape Point



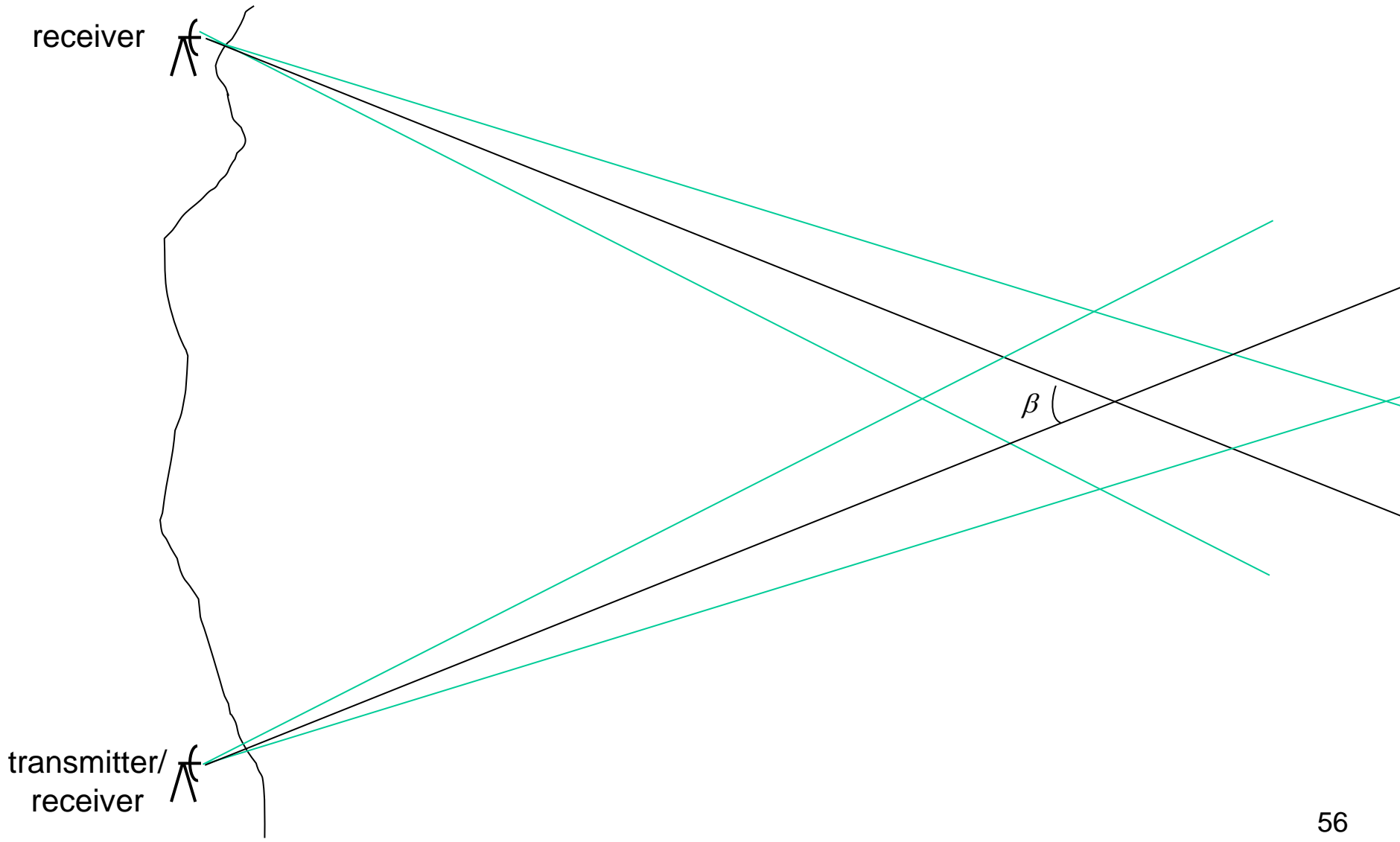
Bistatic clutter trials: Cape Point



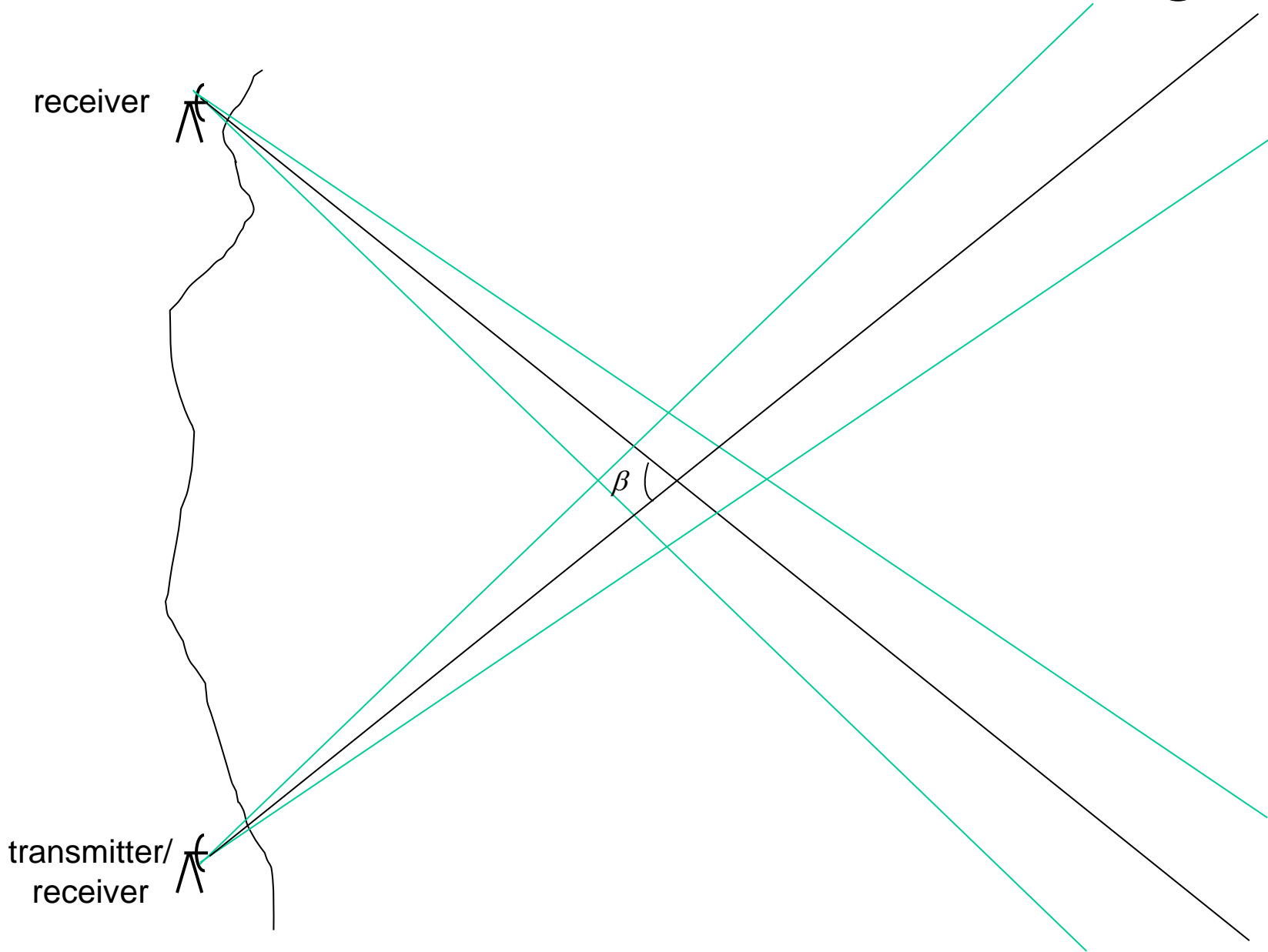
Bistatic clutter trials: Cape Point



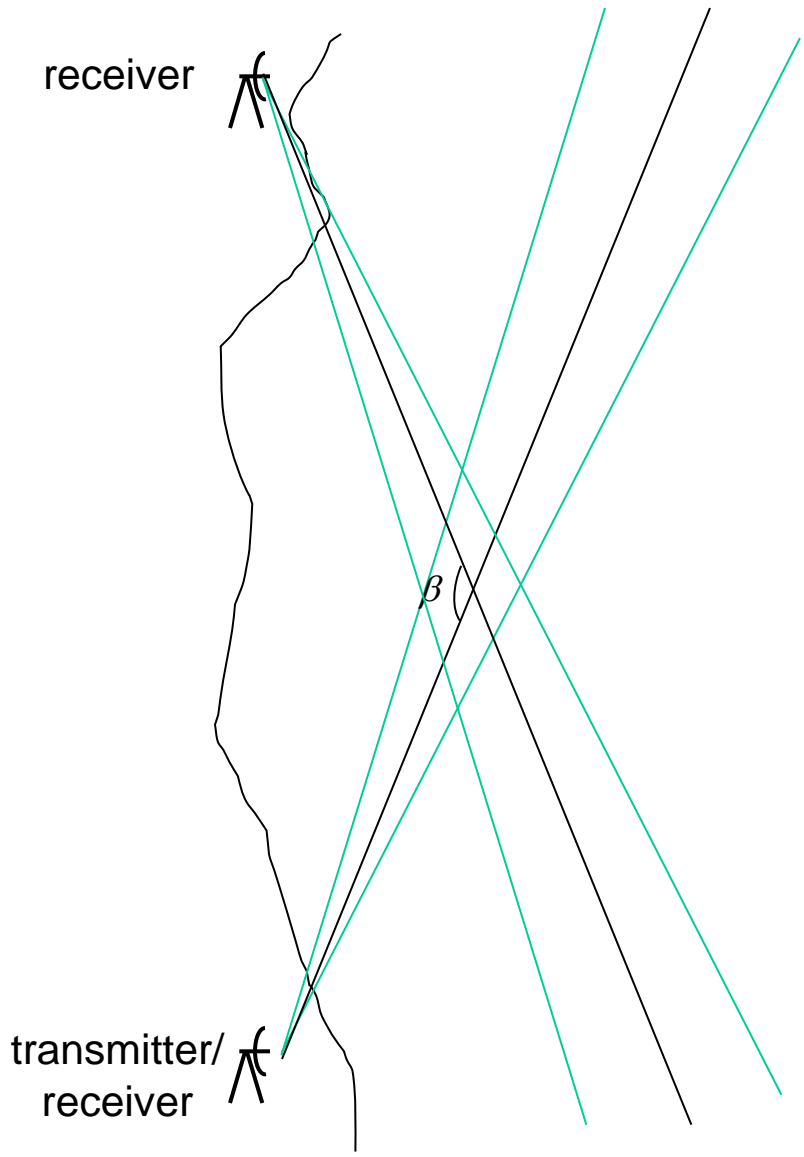
Bistatic clutter trials: Scarborough



Bistatic clutter trials: Scarborough



Bistatic clutter trials: Scarborough



Bistatic clutter trials: Scarborough



Bistatic clutter trials: Scarborough



Bistatic clutter trials: Scarborough

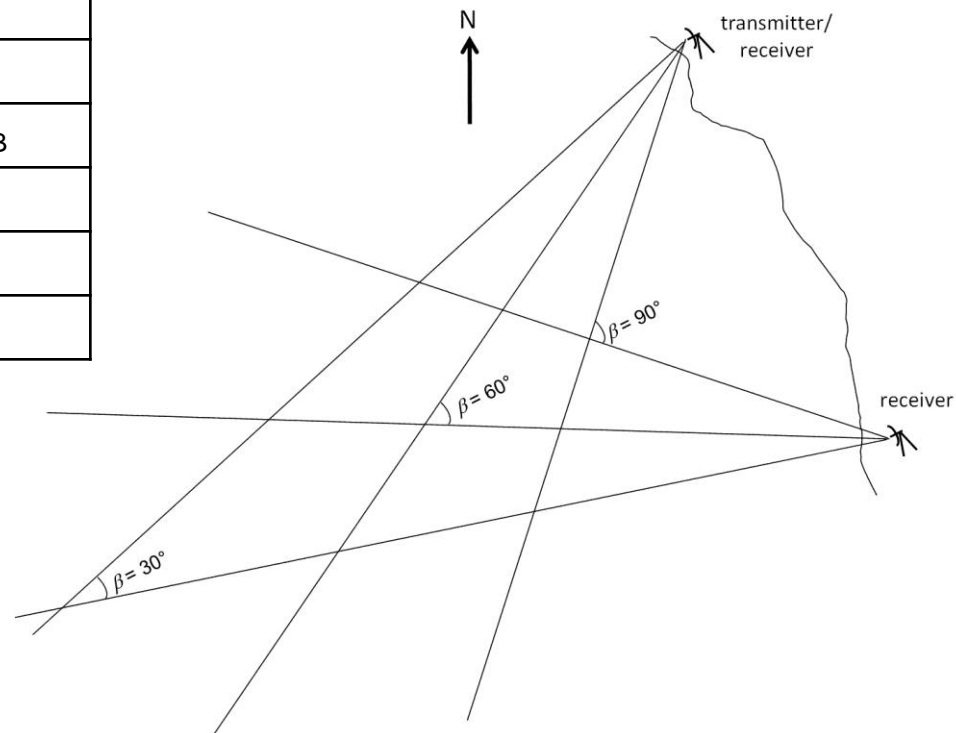


V-pol clutter measurements, 5 October 2010

Parameter	Monostatic Node	Bistatic Node
Carrier Frequency	2.4 GHz	2.4 GHz
Nominal Bandwidth	50 MHz	50 MHz
Beamwidth	9° (az) × 11° (el)	9° (az) × 11° (el)
Height above sea level	12 m	10 m
Rx losses and Noise Figure	7.7 dB	5.4 dB
Tx losses	2 dB	-
Transmitted Power	500 W	-
PRF	1 kHz	-

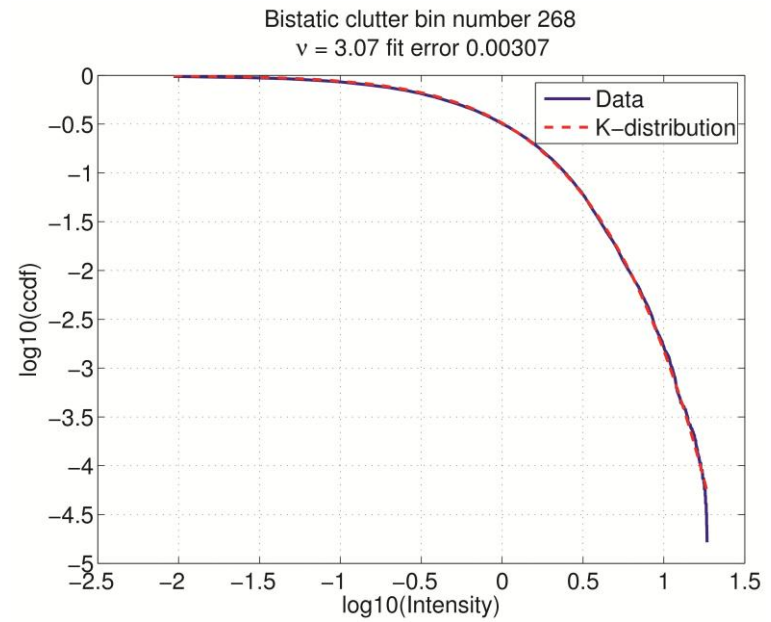
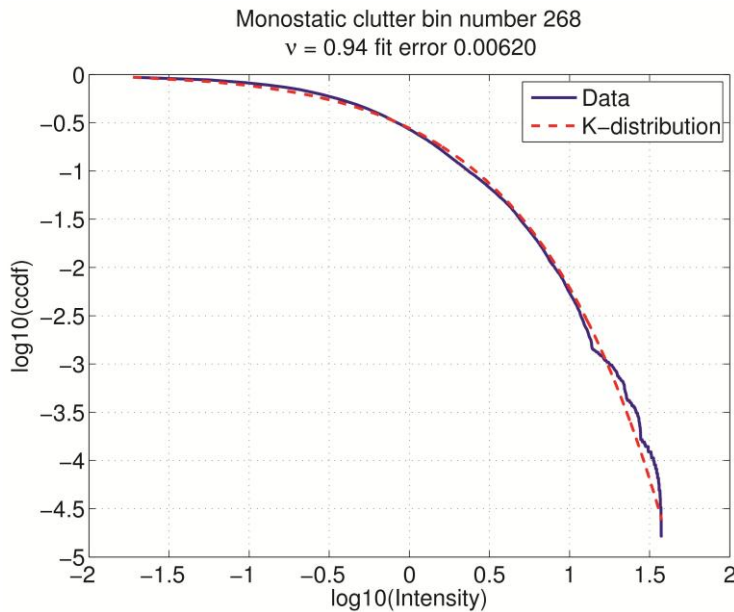
K+noise distribution:

$$P_{C+N}(I) = \int_0^{\infty} \frac{b^\nu x^{\nu-1}}{\Gamma(\nu)} \frac{\exp(bx)}{x + p_n} \exp\left(\frac{-I}{x + p_n}\right) dx$$



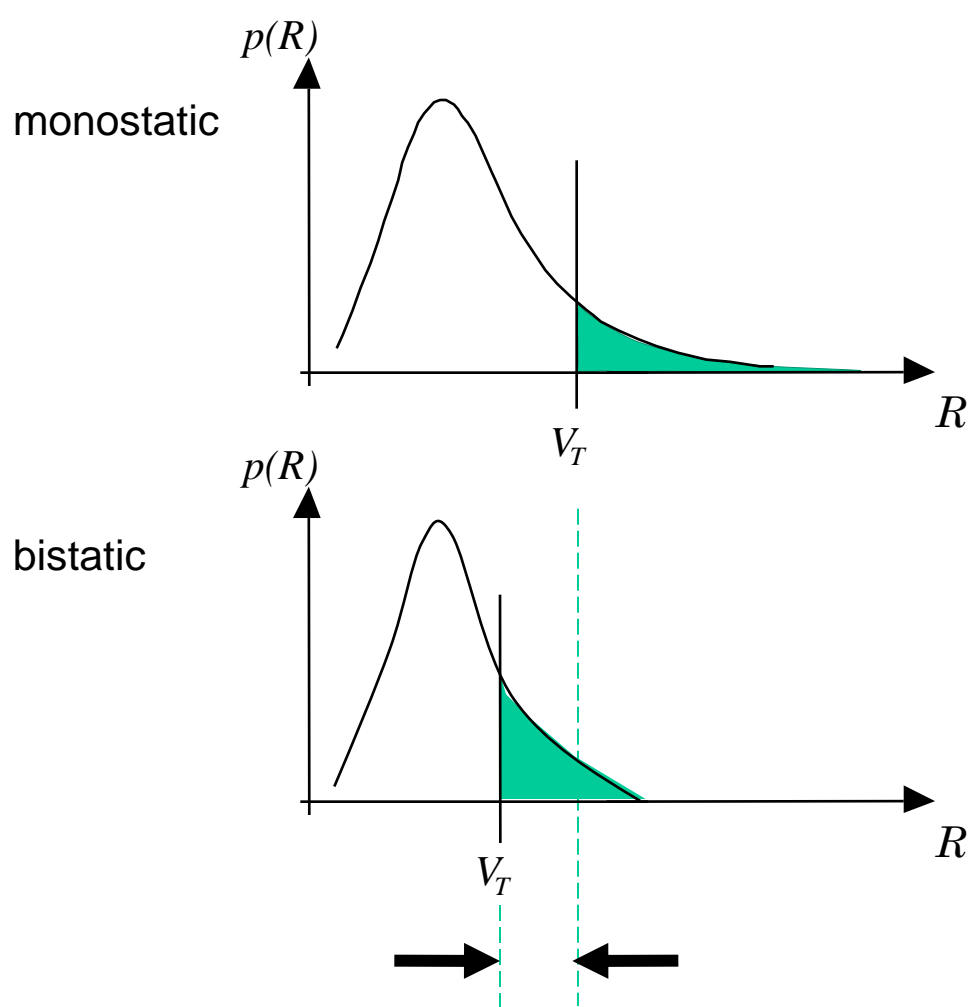
- significant wave height 1.3 m
- swell propagating towards shore,
- sea state 2/3
- wind speed approximately 4 ms^{-1} from a southerly direction.

V-pol clutter measurements, 5 October 2010



$R_M \text{ m}$	β	$\sigma^0_M \text{ dB m}^2/\text{m}^2$	$\sigma^0_B \text{ dB m}^2/\text{m}^2$	CNR M dB	CNR B dB	v_M	v_B
805	30°	-59.2	-58.7	18.1	21.5	0.93	3.11
417	60°	-47.1	-47.6	36.9	40.2	0.22	0.48
295	90°	-44.1	-55.8	41.1	35.6	0.17	1.04

Effect on detection performance



$$P_{FA} = \int_{V_T}^{\infty} p(R)_{\text{clutter+noise}} dR$$

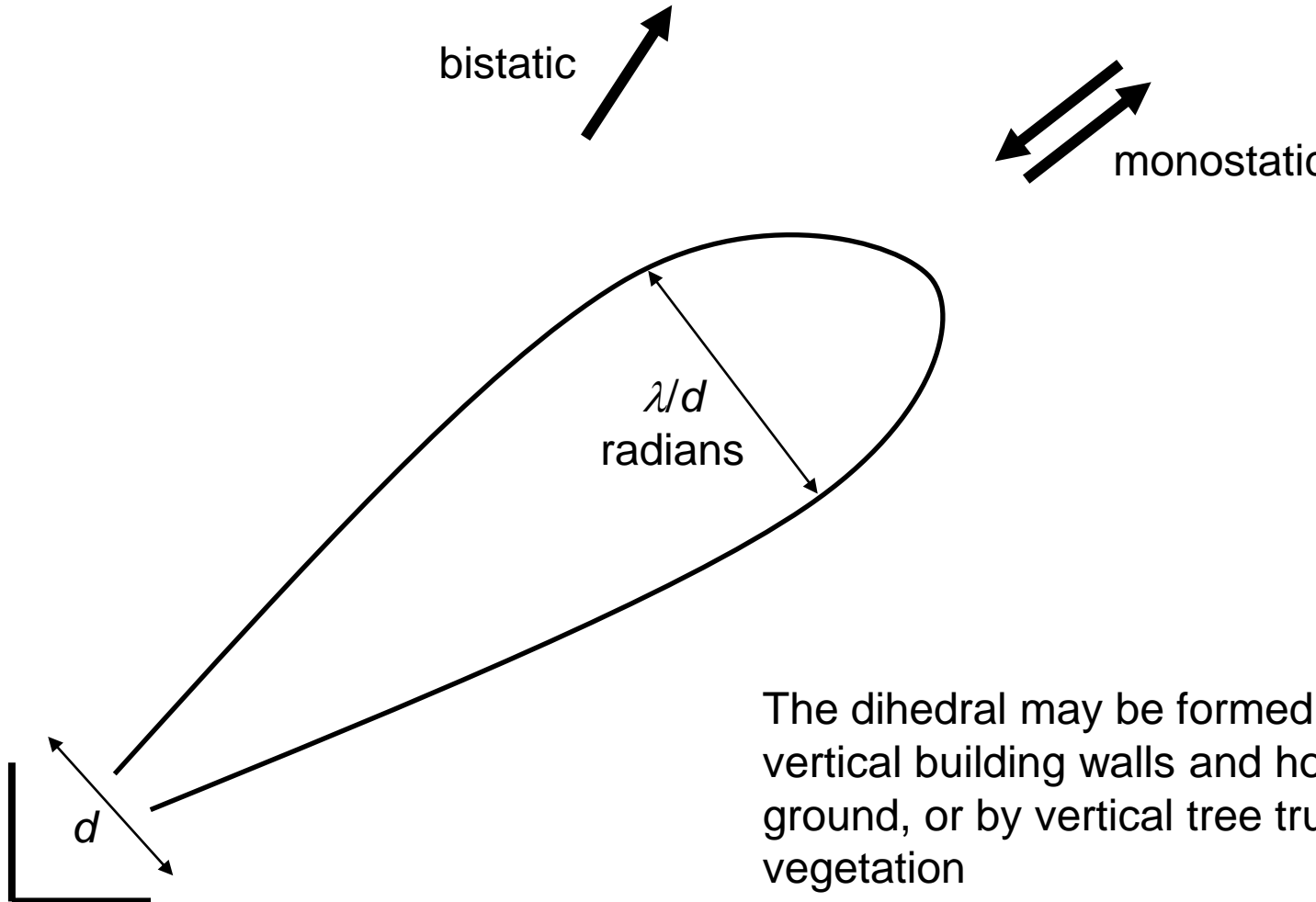
A CFAR algorithm will set a detection threshold to give a particular value of P_{FA} on the basis of clutter+noise.

If the pdf of clutter+noise is shorter-tailed, the detection threshold for a given value of P_{FA} will be lower.

Urban land clutter at PBR frequencies ?

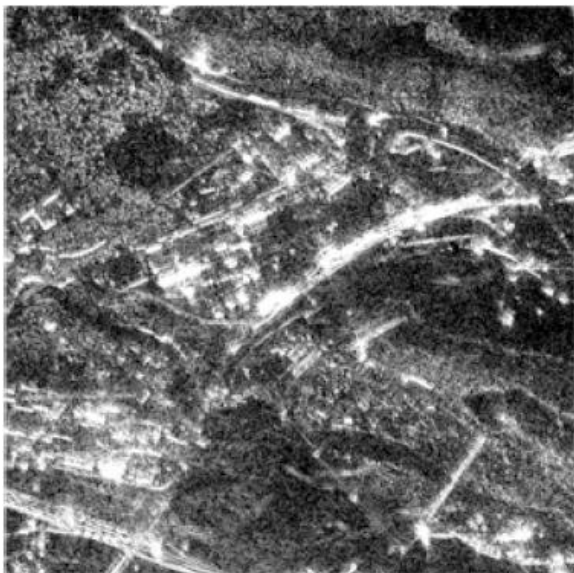
- Urban clutter will contain right-angled features which behave as dihedrals or trihedrals. These will be many wavelengths in size.
- We have some examples of monostatic and bistatic urban clutter at X-band, which show strong monostatic scatter from such features
- At PBR frequencies (VHF and UHF) the scattering from these targets will be broader in angular extent than at X-band
- It should be possible to estimate the properties of clutter from the coefficients of the adaptive filters that suppress the direct signal and multipath
- Also, the wealth of measurements and modelling of urban propagation (multipath) at comms frequencies should allow the clutter properties to be estimated

Urban land clutter at PBR frequencies ?

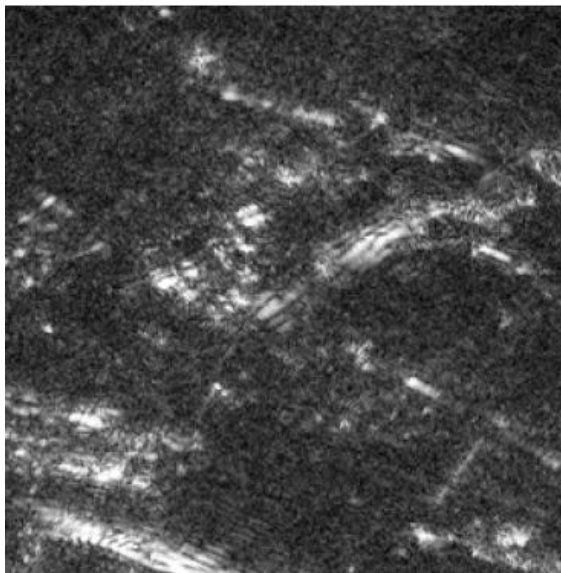


Forested land clutter at HF/UHF frequencies

Similar effects have been observed with bistatic measurements of forested areas using the Swedish CARABAS system (20 – 90 MHz). Here, the dihedral is formed by the vertical trunk of trees and the horizontal ground, though the ratio of dihedral size to wavelength is smaller.



monostatic



bistatic

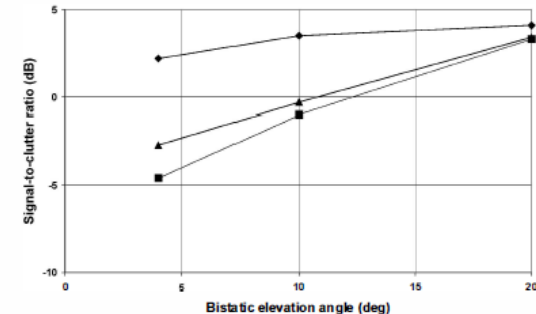


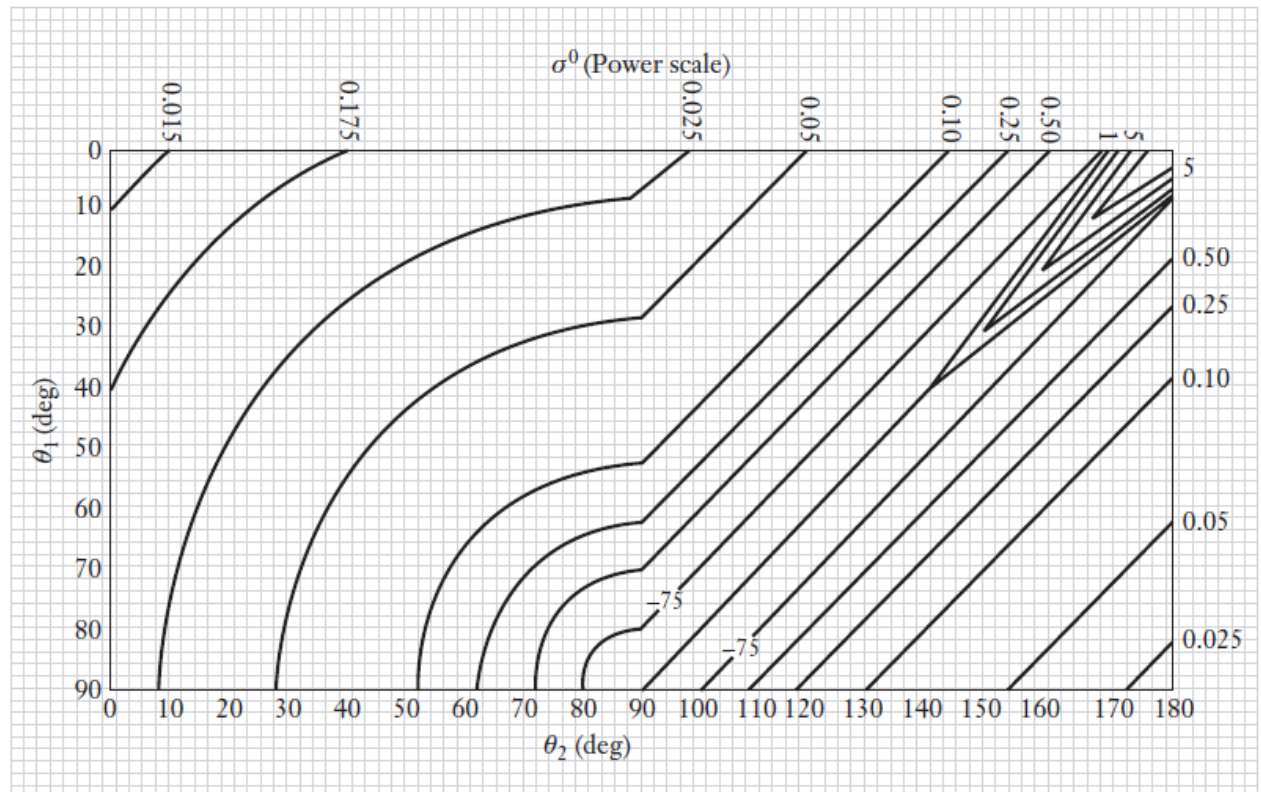
Figure 8 Signal-to-clutter ratio for a truck compared to three different urban clutter areas and measured in the bistatic VHF-band SAR images. Image noise power has been estimated and subtracted from both the truck and clutter measurements.

Ulander, L. et al., 'Bistatic experiment with ultra-wideband VHF-band synthetic aperture radar', EUSAR conference 2008, Friedrichshafen, 2-5 June 2008.

Barmettler, A., Zuberbüler, L., Meier, E., Ulander, L., Gustavsson, A. and Wellig, P., 'Swiss airborne monostatic and bistatic dual-pol SAR experiment at the VHF band', EUSAR conference 2008, Friedrichshafen, 2-5 June 2008.

Bistatic clutter

urban land,
X-band,
VV polarisation

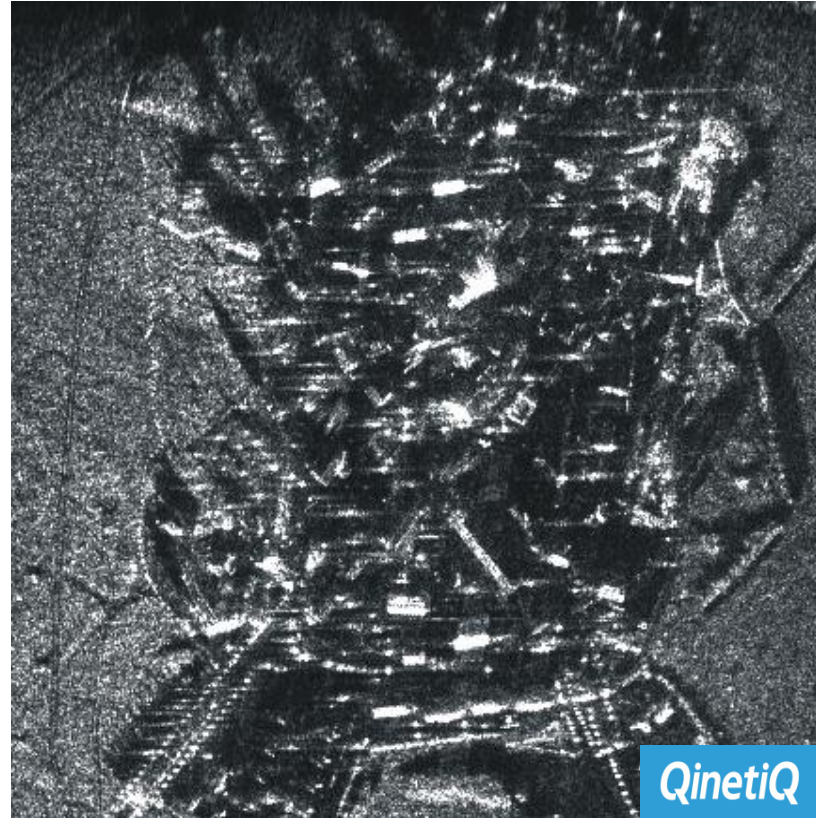


Comparison of monostatic and bistatic SAR



QinetiQ

Monostatic



QinetiQ

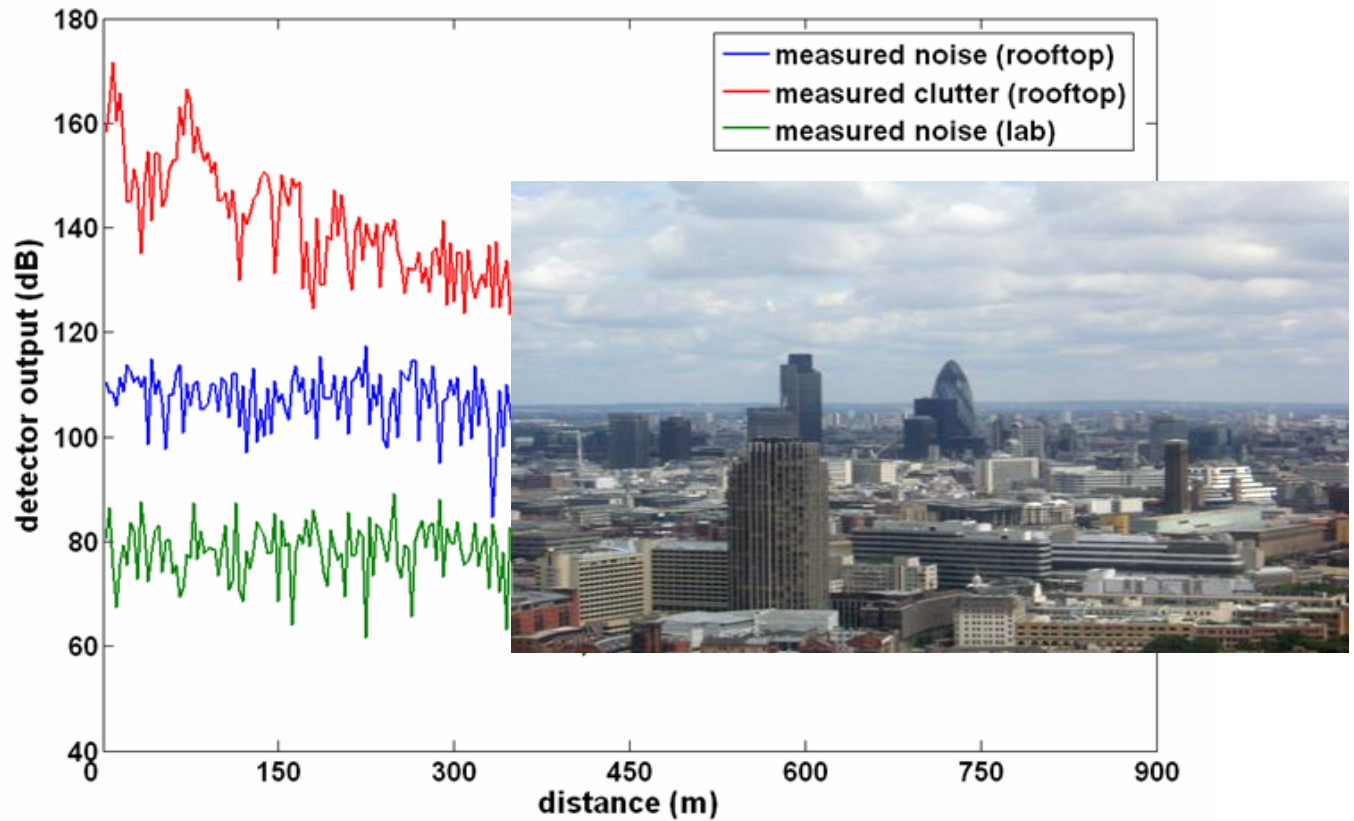
Bistatic
(~70°)

Initial monostatic testing

Initial tests were taken in an urban clutter environment, in the area surrounding UCL

Both noise and clutter measurements were taken

Typical range profile



Initial monostatic testing



Summary

(from chapter 9 of *Advances in Bistatic Radar* – M. Weiner)

1. The clutter cell area for the resolution time-limited case (limited by the receiver resolution time and the transmitter or receiver main lobe beam width) at low grazing angles is more than 30 dB larger in the forward-scattered direction than in the backscattered direction but is less than 10 dB larger for azimuthal angles as large as 135° from the backscattered direction.
2. The surface clutter radar cross section (RCS) is significantly larger in the forward scattered direction than in the backscattered direction and may nullify any advantages of a possibly enhanced target RCS in the forward-scattered direction, particularly at frequencies greater than 300 MHz.
3. Bistatic radar surveillance at an azimuthal angle of approximately 90° from the backscattered direction offers a potential reduction of surface clutter return compared to that from a monostatic radar, based on measurements of selected vegetative and soil themes.

Summary

4. The bistatic surface clutter return at an azimuthal angle as large as 45° from the backscattered direction is not appreciably different from that in the backscattered direction.
5. The definition of clutter cross section per unit area which is used in determining experimental values may give different values from the definition used in theoretical modelling, depending on the type of averaging performed by the latter. The former definition is useful in characterizing *diffuse scatter* (rays reflected in all directions) from rough *extended surfaces* (surfaces that extend beyond the field of view of the transmitter or receiver) whereas the latter definition was originally used to characterize scattering from nonextended surfaces.

Summary

6. Terrain and sea scatter are generally from extended surfaces. Consequently, the number of Fresnel zones subtended by the clutter cell at the receiver or transmitter is usually more than one Fresnel zone. Theoretical models of clutter cross section per unit area from extended surfaces should therefore be evaluated for the corresponding Fresnel zone of the clutter cell. However, for zero-mean stochastic processes, the effect of surface roughness on the expected value of the *coherent component* (proportional to the product of the expected values of the scattered field times the expected value of its phase conjugate) of clutter cross section per unit area is independent of the number of Fresnel zones subtended by the clutter cell at the receiver.

Summary

7. Terrain and sea scatter are generally from extended surfaces. Consequently, the number of Fresnel zones subtended by the clutter cell at the receiver or transmitter is usually more than one Fresnel zone. Theoretical models of clutter cross section per unit area from extended surfaces should therefore be evaluated for the corresponding Fresnel zone of the clutter cell. However, for zero-mean stochastic processes, the effect of surface roughness on the expected value of the *coherent component* (proportional to the product of the expected values of the scattered field times the expected value of its phase conjugate) of clutter cross section per unit area is independent of the number of Fresnel zones subtended by the clutter cell at the receiver.
8. Although various models (semiempirical, geometrical, and statistical) have been made of surface scatter on the basis of various assumptions about the characteristics of the surface, meaningful results are difficult to achieve except over a relatively narrow range of elevation or out-of-plane angles.
9. The existing open literature database of the bistatic scattering coefficient for terrain and sea scatter is from 9 principal investigators over the period 1965–2002.

Summary

10. The most substantial bistatic scattering coefficient data, in terms of number of independent samples, number of terrain and sea themes, number of data curves, or statistical properties, are given by Cost and Peake, Pidgeon, Domville, Larsen and Heimiller, Ewell and Zehner, Ulaby, and McLaughlin.
11. The Bistatic-Monostatic Equivalence Theorem, when applied to target RCSs or extended surfaces, is generally not valid except for small bistatic angles. However, Willis has successfully used the theorem to interpolate the measured database of Domville (for in-plane scatter from rural land, forest, and urban land) to bistatic angles as large as 135° provided that either the incident or scattering angle was less than 5° .
12. Future efforts in expanding the database of the bistatic scattering coefficient should include measurements as a function of cell area to determine homogeneity of the surface theme and to determine whether the scattering coefficient is predominantly coherent or incoherent.

References

- E. Jakeman and P. Pusey, 'A model for non-Rayleigh sea echo', *IEEE Trans. Antennas and Propagation*, vol. 24, no. 6, pp. 806–814, Nov 1976.
- M.M. Horst, F.B. Dyer, M.T. Tuley, 'Radar sea clutter model', *Proc. IEEE Int. Conf. on Antennas and Propagation*, pp6-10, November 1978.
- K.D. Ward, 'Compound representation of high-resolution sea clutter', *Electronics Letters*, Vol.17, No.16, pp561-562, 6 August 1981.
- K.D. Ward and S. Watts, 'Radar sea clutter', *Microwave Journal*, June 1985, pp109-121.
- S. Watts, 'Radar detection prediction in K-distributed sea clutter and thermal noise', *IEEE Trans. Aerospace and Electronic Systems*, Vol.AES-23, No.1, pp40-45, January 1987.
- K.D. Ward, C.J. Baker and S. Watts, 'Maritime surveillance radar, part 1: radar scattering from the ocean surface; part 2: detection performance in sea clutter', *IEE Proc.*, Vol.137, Pt.F, No.2, pp51-62; pp63-72, April 1990.

Further reading

Long, M.W., *Radar Reflectivity of Land and Sea*, Artech House,

Sekine, M. and Mao, Y., *Weibull Radar Clutter*, Peter Peregrinus, 1990.

Billingsley, B., *Low-angle Radar Land Clutter*, Peter Peregrinus/SciTech, 2002.

Curry, G.R., *Radar System Performance Modeling* (second edition), Artech House, 2005.

Ward, K.D., Tough, R.J.A. and Watts, S., *Sea Clutter: Scattering, the K-Distribution and Radar Performance*, IET, London, 2006.